Finite volume methods for multi-component Euler equations with source terms in networks

Alfredo Bermúdez, Xián López and M. Elena Vázquez-Cendón

Universidade de Santiago de Compostela (USC)
Instituto Tecnológico de Matemática Industrial (ITMATI)

Purple SHARK-FV – Ofir, Portugal.

May 15-19 2017

Motivation

- To develop a software to simulate and optimize a gas transportation network, provided with a graphical user interface and a data basis to manage scenarios and results.
- GANESO® (Gas Network Simulation and Optimization).
- Mostly funded by Reganosa Company (Mugardos, Galicia, Spain).

USC UNIVERSIDADE DE SANTIAGO DE COMPOSTELA

Grupo de Investigación en Ingeniería Matemática

Spanish gas transportation network

The goal

- The framework of this talk is transient mathematical modelling of gas transport networks.
- The model consists of a system of nonlinear hyperbolic partial differential equations coupled at the nodes of the network.
- The edges of the graph represent pipes where the gas flow is modelled by the non-isothermal non-adiabatic Euler compressible equations for real gases, with source terms arising from heat transfer with the outside of the network, wall viscous friction, and gravity force; the latter involves the slope of the pipe.

The goal

- Up to now, the gas is assumed to be homogeneous in composition.
- Now, let us suppose that the composition is different from one entry point to another.
- Furthermore, we also assume that, at each entry point, the composition changes along the time.
- Under these assumptions the gas composition in the network changes from point to point and also along the time.
- From the composition, the "gas quality" in terms of its calorific value can be computed at each point x and time t.

USC UNIVERSIDADE DE SANTIAGO DE COMPOSTELA

Grupo de Investigación en Ingeniería Matemática

OUTLINE

- Mathematical model of gas flow in a pipe
- Numerical solution. Finite volume discretization
- Flux and source terms upwinding
- Numerical tests: analytical solution
- Numerical results *vs* experimental data

Modelling one single pipe: Geometry and gravity force term

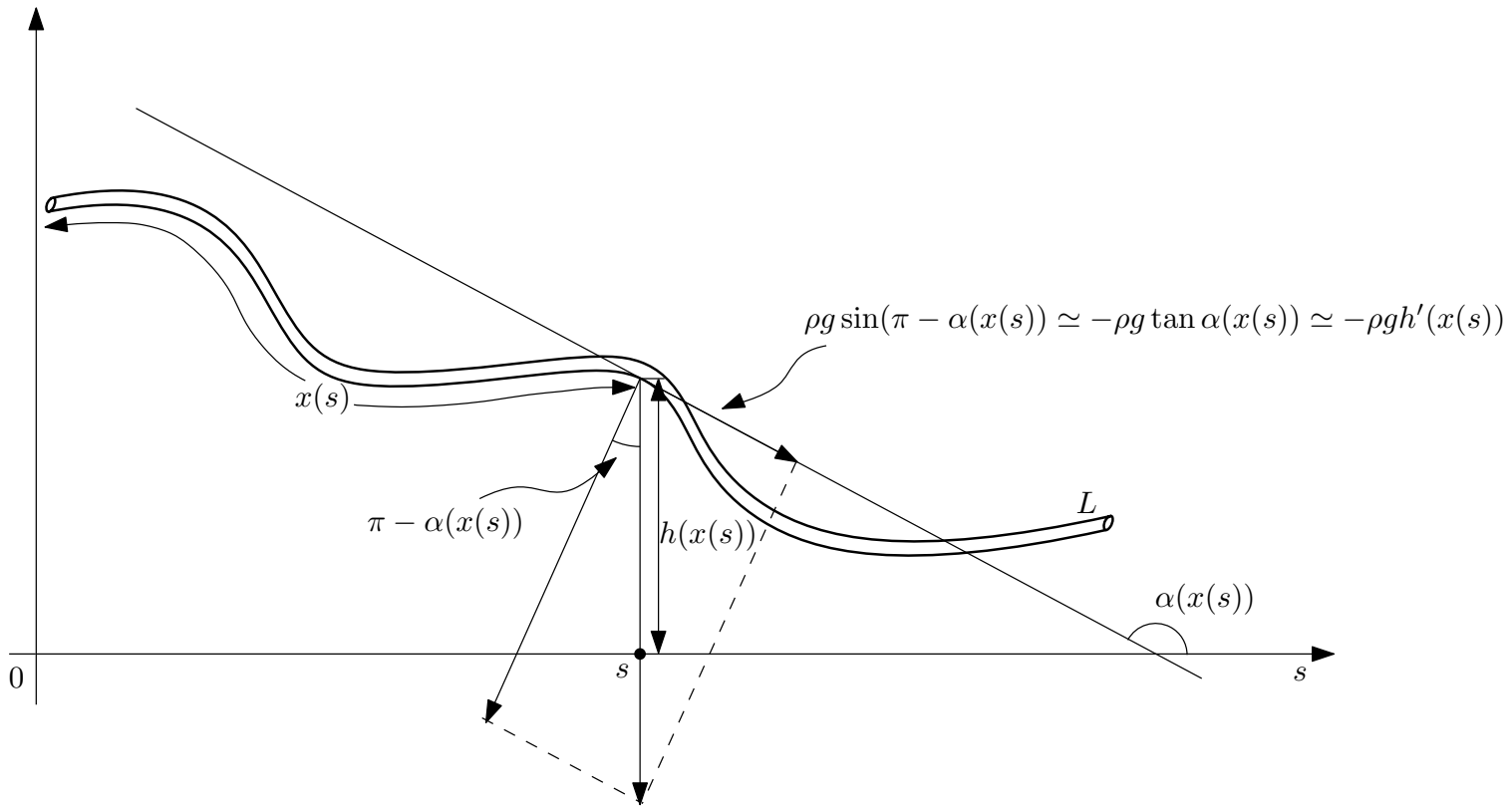

Figure: Approximation of the gravity force term assuming $x'(s) \approx 1$.

Modelling one single pipe: Notations

- ρ is the average mass density (kg/m^3),
- v is the mass-weighted average velocity on cross-sections of the pipe sections (m/s),
- p is the average thermodynamic pressure (N/m^2),
- g is the gravity acceleration (m/s^2),
- h is the height of the pipe at the x cross-section (m),
- D is the diameter of the pipe (m),
- λ is the friction factor between the gas and the pipe walls; it is a non-dimensional number depending on the diameter of the pipe, the rugosity of its wall and the Reynolds number of the flow,

USC UNIVERSIDADE DE SANTIAGO DE COMPOSTELA

Grupo de Investigación en Ingeniería Matemática

Modelling one single pipe: Notations

- E is the average specific total energy (J/kg),
- e is the specific internal energy (J/kg),
- β is a heat transfer coefficient (W/m^{2}K),
- θ is the average temperature (K),
- θ_{ext} is the exterior temperature (K),
- Y_k is the mass fraction of the k-th species,
- $\rho_k = \rho Y_k$ is partial density of the k-th specie (kg/m^3).

USC UNIVERSIDADE DE SANTIAGO DE COMPOSTELA

Grupo de Investigación en Ingeniería Matemática

Modelling one single pipe: Balance law

The balance equations can be rewritten in the compact form:

Euler system:

$$\frac{\partial \mathbf{W}}{\partial t}(x,t) + \frac{\partial \boldsymbol{\mathcal{F}}^{W}}{\partial x}(\mathbf{W}(x,t), \boldsymbol{\rho}(x,t)) = \sum_{j=1}^{3} \boldsymbol{\mathcal{G}}_j(x,t,\mathbf{W}(x,t), \boldsymbol{\rho}(x,t)), \quad (1)$$

Gas composition system:

$$\frac{\partial \boldsymbol{\rho}}{\partial t}(x,t) + \frac{\partial \boldsymbol{\mathcal{F}}^{\rho}}{\partial x}(\mathbf{W}(x,t), \boldsymbol{\rho}(x,t)) = \mathbf{0}, \quad (2)$$

A. Bermúdez, X. López and MEVC, Finite volume methods for multi-component Euler equations with source terms, *Submitted to Computers & Fluids,* (2016).

USC UNIVERSIDADE DE SANTIAGO DE COMPOSTELA

Grupo de Investigación en Ingeniería Matemática

Modelling one single pipe: Balance law

- Conservative variables Euler system: $\mathbf{W} = (W_1, W_2, W_3)$
  - $W_1 = \rho$ (mass density, kg/m^3),
  - $W_2 = \rho v$ (mass flux or linear momentum density, kg/(m^{2}s)),
  - $W_3 = \rho E$ (total energy density, J/m^3),
- Conservative variables gas composition system: $\boldsymbol{\rho} = (\rho_1, \cdots, \rho_{N_e})^t$
  - $\rho_k = \rho Y_k$ (partial density of the k-th species (kg/m^3)),
- Coupling: $W_1 = \sum_{k=1}^{N_e} \rho_k$ then it is enough to solve $N_e - 1$ equations for the species in gas composition system.

Physical flux Euler system

$$\boldsymbol{\mathcal{F}}^W(\mathbf{W}, \boldsymbol{\rho}(x,t)) = \begin{pmatrix} W_2 \\ \frac{W_2^2}{W_1} + \hat{p}(\mathbf{W}, \boldsymbol{\rho}) \\ \left(W_3 + \hat{p}(\mathbf{W}, \boldsymbol{\rho})\right) \frac{W_2}{W_1} \end{pmatrix},$$

Physical flux gas composition system

$$\boldsymbol{\mathcal{F}}^{\rho}(\mathbf{W}(x,t), \boldsymbol{\rho}) = \frac{W_2}{W_1} \boldsymbol{\rho},$$

State equations. Homogeneous mixture of perfect gases

$\hat{p}$ and $\hat{\theta}$ are the mappings giving pressure and absolute temperature from the conservative variables, through the state equations:

$$p = \left(\sum_{k=1}^{N_e} \frac{\rho_k}{M_k} \right) \mathcal{R}\theta, \tag{3}$$

$$\sum_{k=1}^{N_e} \rho_k \int_{\theta_{ref}}^{\theta} \hat{c}_{vk}(s)\, ds = W_3 - \frac{1}{2}\frac{W_2^2}{W_1} - W_1 \hat{e}(\theta_{ref}). \tag{4}$$

- $\hat{e}(\theta_{ref})$ is the specific internal energy at reference temperatures θ_{ref},
- $\hat{c}_{vk}(\theta)$ is the specific heat at constant volume of the k-th species, at temperature θ (J/(kgK)),
- $\mathcal{R}$ is the universal gas constant (J/(k-mol K).

Source terms

Friction: $\mathcal{G}_1(x,t,\mathbf{W}(x,t),\boldsymbol{\rho}(x,t)) = \begin{pmatrix} 0 \\ -\dfrac{\lambda(x,t)}{2D}\dfrac{W_2|W_2|}{W_1} \\ 0 \end{pmatrix},$

Variable height along the pipeline: $\mathcal{G}_2(x,t,\mathbf{W}(x,t),\boldsymbol{\rho}(x,t)) = \begin{pmatrix} 0 \\ -gW_1h'(x) \\ -gW_2h'(x) \end{pmatrix},$

Heat exchange with the exterior:

$$\mathcal{G}_3(x,t,\mathbf{W}(x,t),\boldsymbol{\rho}(x,t)) = \begin{pmatrix} 0 \\ 0 \\ \dfrac{4\beta}{D}\left(\theta_{ext}(x,t) - \hat{\theta}(x,t,\mathbf{W})\right) \end{pmatrix},$$

USC UNIVERSIDADE DE SANTIAGO DE COMPOSTELA

Grupo de Investigación en Ingeniería Matemática

Initial conditions

$$\mathbf{W}(x,0) = \mathbf{W}_0(x), \quad \boldsymbol{\rho}(x,0) = \boldsymbol{\rho}_0(x), \quad x \in (0, \mathcal{L}).$$

- In practice, initial values for density, velocity, temperature and mass fraction of the species at each cross-section x of the pipeline are given, denoted by $\rho_0(x)$, $v_0(x)$, $\theta_0(x)$ and $Y_{k0}(x)$, $k = 1, \cdots, N_e$:

$$W_{10}(x) = \rho_0(x), \; W_{20}(x) = \rho_0(x) v_0(x),$$
$$\rho_k(x,0) = \rho_0(x) Y_{k0}(x), \; k = 1, \cdots, N_e,$$

and $W_{30}(x)$, can be computed by

$$W_{30}(x) = \rho_0(x)\hat{e}(\theta_{ref}) + \sum_{k=1}^{N_e} \rho_{k0}(x) \int_{\theta_{ref}}^{\theta} \hat{c}_{vk}(s)\, ds + \frac{1}{2}\rho_0(x)(v_0(x))^2.$$

Boundary conditions

They are written at the left-end of the pipe, $x = 0$.

- Inflow ($W_2(0,t) > 0$):
  $W_2(0,t) = q_L(t)$, $\theta(0,t) = \theta_L(t)$, $Y_i(0,t) = Y_{iL}(t)$, $i = 1, \cdots, N$.

- Outflow ($W_2(0,t) < 0$): $W_2(0,t) = q_L(t)$,
  $q_L(t)$ is the mass flux ($kg/(m^2 s)$) at $x = 0$ and time t.

- Free exit: $\dfrac{\partial W_i}{\partial x} = 0$, $i = 1, 2, 3$, $\dfrac{\partial Y_k}{\partial x} = 0$, $k = 1, \cdots, N_e$.

- Inlet/Outlet pressure: $p(0,t) = p_L(t)$;
  besides,
  $\theta(0,t) = \theta_L(t)$, $Y_i(0,t) = Y_{iL}(t)$, $i = 1, \cdots, N$ if $W_2(0,t) > 0$.

- Wall: $W_2(0,t) = 0$.

USC UNIVERSIDADE DE SANTIAGO DE COMPOSTELA

mat+i Grupo de Investigación en Ingeniería Matemática

Numerical solution. Constant gas composition

- Euler explicit for time discretization.
- Finite volume method for space discretization.
- Approximate Riemann solver (van Leer's Q-Scheme).
- Upwind discretization of source terms following the general methodology from: A. Bermúdez and MEVC, Upwind methods for hyperbolic conservation laws with source terms, *Comput. and Fluids* 23(8), 1049–1071 (1994).
- More details: A. Bermúdez, X. López and MEVC, Numerical solution of non-isothermal non-adiabatic flow of real gases in pipelines, *J. Comput. Phys.*, 323, 126–148 (2016).

USC UNIVERSIDADE DE SANTIAGO DE COMPOSTELA

Grupo de Investigación en Ingeniería Matemática

Some related work

Well-balanced schemes for a similar problem, Euler equations with gravitation, have introduced by several authors in the last years:

- C. Chalons, F. Coquel, E. Godlewski, P. A. Raviart, M^3AS (2010)
- P. Chandrashekar, C. Klingenberg, SIAM J. Sci. Comput.(2015).
- V. Desveaux, M. Zenk, C. Berthon, C. Klingenberg, Int. J. Numer. Meth. Fluids (2010).
- R. Käppeli, S. Mishra, J. Comput. Phys. (2014).
- J. Luo, K. Xu,N. Liu, SIAM J. Sci. Comput. (2011).
- K. Xu, J. Luo, S. Chen, Adv. Appl. Math. Mech. (2010).
- Y. Xing and C.-W. Shu, J. Sci. Comput. (2013).

USC UNIVERSIDADE DE SANTIAGO DE COMPOSTELA

Grupo de Investigación en Ingeniería Matemática

Numerical solution. Variable gas composition

Physical flux is also space dependent. For a similar problem in shallow water equations, several authors have introduced different numerical methods in the last years:

- P. García-Navarro and MEVC, Comput. and Fluids (2000)
- M.J. Castro, E. D. Fernández-Nieto, T. Morales de Luna, G. Narbona-Reina and C. Parés, M2AN (2013)

Numerical solution. Variable gas composition

To preserve the mass fractions positivity, several authors have introduced different numerical methods in the last years:

- B. Larrouturou, [Research Report] RR-1080, 1989. J. Comput. Phys., (1991)
- L. Cea and MEVC, J. Comput. Phys. (2012)
- S. Paván, J.-M. Hervouet, M. Ricchiuto, R. Ata, J. Comput. Phys. (2016)

- Let us notice first that Euler system and gas composition system are coupled:
  - Pressure and temperature in the former depends on gas composition
  - Velocity (which is given by W_2/W_1) appears in the flux term of the second system
- In this work we are interested in segregated schemes, i.e., in solving the two systems independently:
  - Solving Euler system we must assume that ρ is a given function of (x, t)
  - Solving gas composition system we must assume that $\mathbf{W}$ is a given function of (x, t).
- This fact leads us to write the above systems in a slightly different form, for the sake of clarity. Let us introduce the following vector functions:

$$\mathbf{F}^W(x, t, \mathbf{W}) := \mathcal{F}^W(\mathbf{W}, \rho(x, t)),$$
$$\mathbf{F}^\rho(x, t, \rho) := \mathcal{F}^\rho(\mathbf{W}(x, t), \rho),$$
$$\mathbf{G}_j(x, t, \mathbf{W}) := \mathcal{G}_j(x, t, \mathbf{W}, \rho(x, t)),\ j = 1, 2, 3.$$

- Then the systems can be rewritten as follows:

$$\frac{\partial \mathbf{W}}{\partial t}(x,t) + \frac{d\boldsymbol{F}^W}{dx}(x,t,\mathbf{W}(x,t)) = \sum_{j=1}^{3} \mathbf{G}_j(x,t,\mathbf{W}),$$

$$\frac{\partial \boldsymbol{\rho}}{\partial t}(x,t) + \frac{d\boldsymbol{F}^\rho}{dx}(x,t,\boldsymbol{\rho}(x,t)) = \mathbf{0},$$

where

$$\frac{d\mathbf{F}^W}{dx}(x,t,\mathbf{W}(x,t)) := \frac{\partial \mathbf{F}^W}{\partial x}(x,t,\mathbf{W}(x,t)) + \frac{\partial \mathbf{F}^W}{\partial \mathbf{W}}(x,t,\mathbf{W}(x,t))\frac{\partial \mathbf{W}}{\partial x}(x,t),$$

$$\frac{d\mathbf{F}^\rho}{dx}(x,t,\boldsymbol{\rho}(x,t)) := \frac{\partial \mathbf{F}^\rho}{\partial x}(x,t,\boldsymbol{\rho}(x,t)) + \frac{\partial \mathbf{F}^\rho}{\partial \boldsymbol{\rho}}(x,t,\boldsymbol{\rho}(x,t))\frac{\partial \boldsymbol{\rho}}{\partial x}(x,t).$$

USC UNIVERSIDADE DE SANTIAGO DE COMPOSTELA

Grupo de Investigación en Ingeniería Matemática

Finite volume mesh for the one-dimensional model

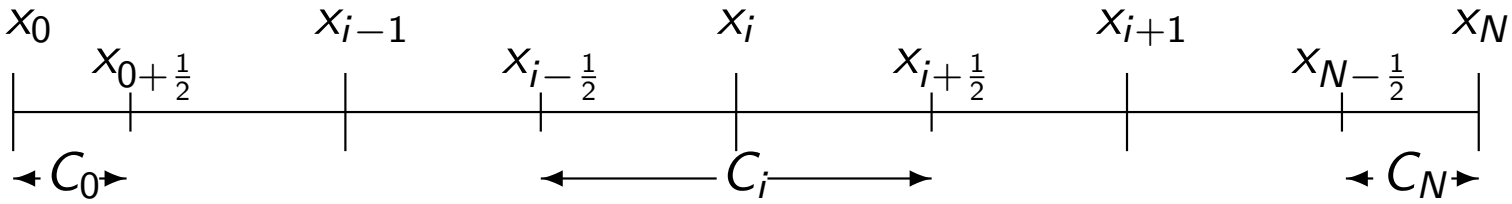

- Let us consider a finite volume mesh of the interval $[0, \mathcal{L}] = [x_0, x_N]$.
- The interior finite volumes are

$$C_i = (x_{i-1/2}, x_{i+1/2}), \ i = 1, \cdots, N-1,$$

where

$$\Delta x = \mathcal{L}/N, \ x_i = i\Delta x \text{ and } x_{i-1/2} = \tfrac{1}{2}(x_{i-1} + x_i), \ i = 1, \cdots, N.$$

- The boundary finite volumes are $C_0 = (x_0, x_{1/2}), \ C_N = (x_{N-1/2}, x_N)$.

USC UNIVERSIDADE DE SANTIAGO DE COMPOSTELA

Grupo de Investigación en Ingeniería Matemática

- By integrating in C_i, $i = 1, \cdots, N-1$, we get

$$\frac{d}{dt}\int_{C_i} \mathbf{W}(x,t)\,\mathrm{d}x + \mathbf{F}^W(x_{i+1/2}, t, \mathbf{W}(x_{i+1/2}, t)) - \mathbf{F}^W(x_{i-1/2}, t, \mathbf{W}(x_{i-1/2}, t)) = \sum_{j=1}^{3}\int_{C_i} \mathbf{G}_j(x,t,\mathbf{W}(x,t))\,\mathrm{d}x.$$

- The approximated solution is taken constant on each finite volume C_i where its value, at time t, is denoted by $\mathbf{W}_i(t)$.
- Therefore, at the boundaries of the finite volumes we approximate the flux at these points by a so-called numerical flux $\mathbf{\Phi}$:

$$\mathbf{F}^W(x_{i-1/2}, t, \mathbf{W}(x_{i-1/2}, t)) \approx \mathbf{\Phi}^W(x_{i-1}, x_i, t, \mathbf{W}_{i-1}(t), \mathbf{W}_i(t)), i = 1, \cdots, N-1$$

- Several numerical fluxes are proposed in the literature to approximate $\mathbf{F}$. We have chosen the Q-scheme of van Leer for which $\mathbf{\Phi}$ is defined by

$$\begin{aligned}\mathbf{\Phi}^W(x_L, x_R, t, \mathbf{W}_L, \mathbf{W}_R) &= \tfrac{1}{2}\left(\mathbf{F}^W(x_L, t, \mathbf{W}_L) + \mathbf{F}^W(x_R, t, \mathbf{W}_R)\right) \\ &\quad -\tfrac{1}{2}|\mathcal{Q}^W(x_L, x_R, t, \mathbf{W}_L, \mathbf{W}_R)|(\mathbf{W}_R - \mathbf{W}_L),\end{aligned}$$

where

$$\mathcal{Q}^W(x_L, x_R, t, \mathbf{W}_L, \mathbf{W}_R) = \frac{\partial \mathbf{F}^W}{\partial \mathbf{W}}\left(\frac{1}{2}(x_L + x_R), t, \frac{1}{2}(\mathbf{W}_L + \mathbf{W}_R)\right).$$

- Let us recall that the absolute value of a diagonalizable matrix Q is $|Q| = X|\Lambda|X^{-1}$, where $|\Lambda|$ is the diagonal matrix of the absolute values of the eigenvalues of Q, and $Q = X\Lambda X^{-1}$.

USC UNIVERSIDADE DE SANTIAGO DE COMPOSTELA

Grupo de Investigación en Ingeniería Matemática

- In order to make a full discretization, a mesh of the time interval is introduced:

$$t_n = n\Delta t, \;\; n = 0, \cdots, M.$$

- Let us denote by $\mathbf{W}_i^n$ the approximation of $\mathbf{W}(x_i, t_n)$ given by the explicit Euler numerical scheme:

$$\frac{\mathbf{W}_i^{n+1} - \mathbf{W}_i^n}{\Delta t} + \frac{1}{\Delta x}\left(\mathbf{\Phi}^W(x_i, x_{i+1}, t_n, \mathbf{W}_i^n, \mathbf{W}_{i+1}^n) - \mathbf{\Phi}^W(x_{i-1}, x_i, t_n, \mathbf{W}_{i-1}^n, \mathbf{W}_i^n)\right)$$
$$= \sum_{j=1}^{3} \mathbf{G}_{j,i}^n, \quad (E1)$$

- $\mathbf{G}_{j,i}^n$ denotes an upwinded approximation of

$$\frac{1}{\Delta x}\int_{C_i}\mathbf{G}_j(x,t_n,\mathbf{W}(x,t_n))\,\mathrm{d}x$$

- Let us introduce the $\mathbf{G}_{j,i}^n$ for $j=1,2,3$. Following Bermúdez and MEVC (1994), we define these approximations by using the functions $\Psi_j,\ j=1,2,3,$ to be given below, as follows:

$$\mathbf{G}_{ji}^n := \Psi_j(x_{i-1},x_i,x_{i+1},t_n,\mathbf{W}_{i-1}^n,\mathbf{W}_i^n,\mathbf{W}_{i+1}^n),\ j=1,2,3.$$

- In order to get a well-balanced scheme, functions Ψ_j are defined in accordance with the chosen numerical flux.
- In our case, we have taken the Q-scheme of van Leer and hence

$$\Psi_j(x,y,z,t,\mathbf{U},\mathbf{V},\mathbf{W}) = \Psi_j^L(x,y,t,\mathbf{U},\mathbf{V}) + \Psi_j^R(y,z,t,\mathbf{V},\mathbf{W}),\ j=1,2,3,$$

- Ψ_j^L and Ψ_j^R are approximations of the integrals $\frac{2}{\Delta x}\int_{x_{i-1/2}}^{x_i} \mathbf{G}_j(x,\mathbf{W}^n)\,\mathrm{d}x$ and $\frac{2}{\Delta x}\int_{x_i}^{x_{i+1/2}} \mathbf{G}_j(x,\mathbf{W}^n)\,\mathrm{d}x$,.

$$\begin{aligned}&\boldsymbol{\Psi}_j^L(x_{i-1},x_i,t_n,\mathbf{W}_{i-1}^n,\mathbf{W}_i^n)\\ &:= \frac{1}{2}\left[I + |\mathcal{Q}_{i-1/2}^{Wn}|(\mathcal{Q}_{i-1/2}^{Wn})^{-1}\right]\hat{\mathbf{G}}_j(x_{i-1},x_i,t_n,\mathbf{W}_{i-1}^n,\mathbf{W}_i^n),\end{aligned}$$

$$\begin{aligned}&\boldsymbol{\Psi}_j^R(x_i,x_{i+1},t_n,\mathbf{W}_i^n,\mathbf{W}_{i+1}^n)\\ &:= \frac{1}{2}\left[I - |\mathcal{Q}_{i+1/2}^{Wn}|(\mathcal{Q}_{i+1/2}^{Wn})^{-1}\right]\hat{\mathbf{G}}_j(x_i,x_{i+1},t_n,\mathbf{W}_i^n,\mathbf{W}_{i+1}^n),\end{aligned}$$

USC UNIVERSIDADE DE SANTIAGO DE COMPOSTELA

Grupo de Investigación en Ingeniería Matemática

Average density

- From the numerical results for static tests given below, we deduce that the best choice of the average density involved in $\mathbf{G}_j$ is this logarithmic average density introduced by Ismail and Roe (2009):

$$\hat{\rho}(\mathbf{W}_L, \mathbf{W}_R) = \begin{cases} \dfrac{\rho_R - \rho_L}{\ln(\rho_R) - \ln(\rho_L)} & \text{if} \quad \rho_R \neq \rho_L, \\ \rho_L & \text{if} \quad \rho_R = \rho_L. \end{cases}$$

- However, the arithmetic average will be also considered, especially for unsteady cases.

The Euler stage. A new segregated scheme ($E2$)

It is well known that this discrete approximation does not work properly in the case of mixtures of gases.

- ? The first term of $\mathbf{\Phi}^W$ leads to a centred scheme of $\mathbf{F}^W(x,t,\mathbf{W})$.
- ? The second part of $\mathbf{\Phi}^W$, $-\frac{1}{2}|\mathcal{Q}^W|(\mathbf{W}_R-\mathbf{W}_L)$ is the numerical viscosity needed for the stability of the scheme. The important remark is that this term is built with the Jacobian matrix $\frac{\partial \mathbf{F}^W}{\partial \mathbf{W}}(x,t,\mathbf{W}(x,t)$ so it only adds artificial viscosity (equivalently, upwinding) to the discretization of the term $\frac{\partial}{\partial \mathbf{W}}\mathbf{F}^W(x,t,\mathbf{W})\frac{\partial}{\partial x}\mathbf{W}$ but not to the discretization of the other term, $\frac{\partial}{\partial x}\mathbf{F}^W(x,t,\mathbf{W}(x,t))$.
- This lack of upwinding causes the bad behaviour of the scheme.

- Therefore, according to the previous analysis, the remedy to the bad behaviour of $E1$ should consist in adding a new artificial viscosity term to get an upwind discretization of $\dfrac{\partial \mathbf{F}^W}{\partial x}(x,t,\mathbf{W}(x,t))$.
- We propose to define this viscosity term as the difference between an upwind and a centred discretization of this partial derivative. This is the underlying idea in the discretization we propose below:

$$\frac{d}{dt}\int_{C_i}\mathbf{W}(x,t)\,\mathrm{d}x+\mathbf{F}^W(x_{i+1/2},t,\mathbf{W}(x_{i+1/2},t))+\mathbf{F}^W(x_{i-1/2},t,\mathbf{W}(x_{i-1/2},t))$$
$$-\int_{C_i}\mathbf{V}(x,t,\mathbf{W}(x,t))\,\mathrm{d}x=\sum_{j=1}^{4}\int_{C_i}\mathbf{G}_j(x,t,\mathbf{W}(x,t))\,\mathrm{d}x.$$

for $i=0,\cdots,N$, where

$$\mathbf{V}(x,t,\mathbf{W}):=\frac{\partial}{\partial x}\mathbf{F}^W(x,t,\mathbf{W}),\ \mathbf{G}_4(x,t,\mathbf{W}):=-\frac{\partial}{\partial x}\mathbf{F}^W(x,t,\mathbf{W})$$

- Let us denote by $\mathbf{W}_i^n$ the approximation of $\mathbf{W}(x_i, t_n)$ given by the explicit Euler method

$$\frac{\mathbf{W}_i^{n+1} - \mathbf{W}_i^n}{\Delta t} + \frac{1}{\Delta x}\left\{\mathbf{\Phi}^W(x_i, x_{i+1}, t_n, \mathbf{W}_i^n, \mathbf{W}_{i+1}^n) - \mathbf{\Phi}^W(x_{i-1}, x_i, t_n, \mathbf{W}_{i-1}^n, \mathbf{W}_i^n)\right\}$$

$$-\mathbf{V}_i^n = \sum_{j=1}^{4} \mathbf{G}_{j,i}^n, \quad (E2)$$

where $\mathbf{V}_i^n := \frac{1}{2}\left(\mathbf{V}_i^{Ln} + \mathbf{V}_i^{Rn}\right)$ denotes a centred approximation and $\mathbf{G}_{4,i}^n$ denotes an upwind approximation of $\frac{1}{\Delta x}\int_{C_i} \mathbf{G}_4(x, t_n, \mathbf{W}^n)\, \mathrm{d}x$.

- $\mathbf{V}_i^n := \frac{1}{2}\left(\mathbf{V}_i^{Ln} + \mathbf{V}_i^{Rn}\right)$, denotes a centred approximation of

$$\frac{2}{\Delta x}\int_{x_{i-\frac{1}{2}}}^{x_i} \mathbf{V}(x, t_n, \mathbf{W}^n)\, \mathrm{d}x + \frac{2}{\Delta x}\int_{x_i}^{x_{i+\frac{1}{2}}} \mathbf{V}(x, t_n, \mathbf{W}^n)\, \mathrm{d}x.$$

- where

$$\mathbf{V}_i^{Ln} \approx \mathbf{V}\left(\frac{x_{i-1}+x_i}{2}, t_n, \frac{1}{2}\left(\mathbf{W}_{i-1}^n + \mathbf{W}_i^n\right)\right)$$

$$\mathbf{V}_i^{Rn} \approx \mathbf{V}\left(\frac{x_i+x_{i+1}}{2}, t_n, \frac{1}{2}\left(\mathbf{W}_i^n + \mathbf{W}_{i+1}^n\right)\right)$$

USC UNIVERSIDADE DE SANTIAGO DE COMPOSTELA

Grupo de Investigación en Ingeniería Matemática

Expression of **V**

- To introduce **V**, we compute, for a mixture of calorically perfect gases, the flux in terms of the conservative variables:

$$\mathbf{F}^W(x,t,\mathbf{W}) = \begin{pmatrix} W_2 \\ (\gamma(x,t)-1)W_3 + \dfrac{(3-\gamma(x,t))}{2}\dfrac{W_2^2}{W_1} \\ \gamma(x,t)\dfrac{W_2W_3}{W_1} + (1-\gamma(x,t))\dfrac{W_2^3}{2W_1^2} \end{pmatrix},$$

where $\gamma(x,t) = \frac{c_p(x,t)}{c_v(x,t)} = \frac{\sum_{k=1}^{N_e} Y_k(x,t)c_{pk}}{\sum_{k=1}^{N_e} Y_k(x,t)c_{vk}}$.

Expression of $\mathbf{V}$

- Then, $\mathbf{V}$ for a mixture of calorically perfect gases is

$$\mathbf{V}(x,t,\mathbf{W}(x,t)) := \frac{\partial}{\partial x}\mathbf{F}^{W}(x,t,\mathbf{W}(x,t))$$

$$= \frac{\partial}{\partial x}\gamma(x,t)\begin{pmatrix} 0 \\ W_3 - \dfrac{W_2^2}{W_1} \\ \dfrac{W_2}{W_1}\left(W_3 - \dfrac{W_2^2}{W_1}\right) \end{pmatrix}.$$

Centred discretization of $\mathbf{V}$

- In order to obtain a well-balanced scheme we deduce that the best choice of the average discretization $\mathbf{V}_i^n := \frac{1}{2}\left(\mathbf{V}_i^{Ln} + \mathbf{V}_i^{Rn}\right)$ is given by

$$V_{2i}^{Ln} = \frac{\gamma_i^n - \gamma_{i-1/2}^n}{\Delta x}\left(W_{3i}^n - \frac{(W_{2i}^n)^2}{2W_{1i}^n}\right) + \frac{\gamma_{i-1/2}^n - \gamma_{i-1}^n}{\Delta x}\left(W_{3(i-1)}^n - \frac{\left(W_{2(i-1)}^n\right)^2}{2W_{1(i-1)}^n}\right),$$

$$V_{2i}^{Rn} = \frac{\gamma_{i+1}^n - \gamma_{i+1/2}^n}{\Delta x}\left(W_{3(i+1)}^n - \frac{\left(W_{2(i+1)}^n\right)^2}{2W_{1(i+1)}^n}\right) + \frac{\gamma_{i+1/2}^n - \gamma_i^n}{\Delta x}\left(W_{3i}^n - \frac{(W_{2i}^n)^2}{2W_{1i}^n}\right).$$

USC UNIVERSIDADE DE SANTIAGO DE COMPOSTELA

Grupo de Investigación en Ingeniería Matemática

Centred discretization of **V**

$$V_{3i}^{Ln} = \frac{\gamma_i^n - \gamma_{i-1/2}^n}{\Delta x}\left(W_{3i}^n - \frac{(W_{2i}^n)^2}{2W_{1i}^n}\right)\frac{W_{2i}^n}{W_{1i}^n} + \frac{\gamma_{i-1/2}^n - \gamma_{i-1}^n}{\Delta x}\left(W_{3(i-1)}^n - \frac{\left(W_{2(i-1)}^n\right)^2}{2W_{1(i-1)}^n}\right)\frac{W_{2(i-1)}^n}{W_{1(i-1)}^n},$$

$$V_{3,i}^{Rn} = \frac{\gamma_{i+1}^n - \gamma_{i+1/2}^n}{\Delta x}\left(W_{3,i+1}^n - \frac{\left(W_{2,i+1}^n\right)^2}{2W_{1,i+1}^n}\right)\frac{W_{2,i+1}^n}{W_{1,i+1}^n} + \frac{\gamma_{i+1/2}^n - \gamma_i^n}{\Delta x}\left(W_{3,i}^n - \frac{(W_{2,i}^n)^2}{2W_{1,i}^n}\right)\frac{W_{2,i}^n}{W_{1,i}^n}.$$

- Let us recall that the first component of **V** is null, and

$$\gamma_{i-1/2}^n = \gamma\left(\frac{x_{i-1}+x_i}{2}, t_n\right),\ \gamma_{i+1/2}^n = \gamma\left(\frac{x_i+x_{i+1}}{2}, t_n\right)$$

USC UNIVERSIDADE DE SANTIAGO DE COMPOSTELA

matti Grupo de Investigación en Ingeniería Matemática

- In summary, the scheme given by $(E2)$ is

$$\mathbf{W}_i^{n+1}=\mathbf{W}_i^n-\frac{\Delta t}{\Delta x}\left\{\mathbf{\Phi}^W(x_i,x_{i+1},t_n,\mathbf{W}_i^n,\mathbf{W}_{i+1}^n)-\mathbf{\Phi}^W(x_{i-1},x_i,t_n,\mathbf{W}_{i-1}^n,\mathbf{W}_i^n)\right\}$$
$$+\frac{\Delta t}{2}\left(\mathbf{V}_i^{Ln}+\mathbf{V}_i^{Rn}\right)+\Delta t\sum_{j=1}^{4}\left(\mathbf{\Psi}_j^L(x_{i-1},x_i,t_n,\mathbf{W}_{i-1}^n,\mathbf{W}_i^n)+\mathbf{\Psi}_j^R(x_i,x_{i+1},t_n,\mathbf{W}_i^n,\mathbf{W}_{i+1}^n)\right)$$

- then we get the purple difference between $(E2)$ and $(E1)$

$$\mathbf{W}_i^{n+1}=\mathbf{W}_i^n-\frac{\Delta t}{\Delta x}\left\{\mathbf{\Phi}^W(x_i,x_{i+1},t_n,\mathbf{W}_i^n,\mathbf{W}_{i+1}^n)-\mathbf{\Phi}^W(x_{i-1},x_i,t_n,\mathbf{W}_{i-1}^n,\mathbf{W}_i^n)\right\}$$
$$-\frac{\Delta t}{2}|\mathcal{Q}_{i-1/2}^{Wn}|(\mathcal{Q}_{i-1/2}^{Wn})^{-1}\mathbf{V}_i^{Ln}+\frac{\Delta t}{2}|\mathcal{Q}_{i+1/2}^{Wn}|(\mathcal{Q}_{i+1/2}^{W,n})^{-1}\mathbf{V}_i^{Rn}$$
$$+\Delta t\sum_{j=1}^{3}\left(\mathbf{\Psi}_j^L(x_{i-1},x_i,t_n,\mathbf{W}_{i-1}^n,\mathbf{W}_i^n)+\mathbf{\Psi}_j^R(x_i,x_{i+1},t_n,\mathbf{W}_i^n,\mathbf{W}_{i+1}^n)\right)$$

USC UNIVERSIDADE DE SANTIAGO DE COMPOSTELA

Grupo de Investigación en Ingeniería Matemática

The gas composition stage. A first segregated scheme (C1)

- A similar problem to the one analyzed above also arises in solving the second block of equations, i.e. gas composition system, but unlike the Euler block they do not include any source term.
- For upwind dicretization the numerical flux is also defined by the Q-scheme of van Leer, that is,

$$\begin{aligned}\mathbf{\Phi}^{\rho}(x_L, x_R, t, \boldsymbol{\rho}_L, \boldsymbol{\rho}_R) = \frac{1}{2}\Big(\mathbf{F}^{\rho}(x_L, t, \boldsymbol{\rho}_L) + \mathbf{F}^{\rho}(x_R, t, \boldsymbol{\rho}_R)\Big) \\ - \frac{1}{2}|\mathcal{Q}^{\rho}(x_L, x_R, t, \boldsymbol{\rho}_L, \boldsymbol{\rho}_R)|(\boldsymbol{\rho}_R - \boldsymbol{\rho}_L),\end{aligned}$$

where

$$\mathcal{Q}^{\rho}(x_L, x_R, t, \boldsymbol{\rho}_L, \boldsymbol{\rho}_R) := \frac{\partial \mathbf{F}^{\rho}}{\partial \boldsymbol{\rho}}\Big(\frac{1}{2}(x_L+x_R), t, \frac{1}{2}(\boldsymbol{\rho}_L+\boldsymbol{\rho}_R)\Big) = v\big(\frac{1}{2}(x_L+x_R), t\big)\mathcal{I},$$

and $\mathcal{I}$ is the identity matrix.

- The corresponding scheme is

$$\frac{\boldsymbol{\rho}_i^{n+1}-\boldsymbol{\rho}_i^n}{\Delta t}+\frac{1}{\Delta x}\left(\boldsymbol{\Phi}^{\rho}(x_i,x_{i+1},t_n,\boldsymbol{\rho}_i^n,\boldsymbol{\rho}_{i+1}^n)-\boldsymbol{\Phi}^{\rho}(x_{i-1},x_i,t_n,\boldsymbol{\rho}_{i-1}^n,\boldsymbol{\rho}_i^n)\right)=\mathbf{0}.\ (C1)$$

- The drawback of this scheme is that it does not satisfy the maximum principle so the discrete partial densities $\rho_{k,i}^n$ can be negative. In order to avoid this inconvenient two different schemes are introduced below.

The gas composition stage. New segregated schemes

- Let us recall that the physical flux term consists of two parts:

$$\frac{d\boldsymbol{F}^{\rho}}{dx}(x,t,\boldsymbol{\rho}(x,t)) = \frac{\partial \mathbf{F}^{\rho}}{\partial x}(x,t,\boldsymbol{\rho}(x,t)) + \frac{\partial \mathbf{F}^{\rho}}{\partial \boldsymbol{\rho}}(x,t,\boldsymbol{\rho}(x,t))\frac{\partial \boldsymbol{\rho}}{\partial x}(x,t)$$
$$= \frac{\partial v}{\partial x}(x,t)\boldsymbol{\rho}(x,t) + v(x,t)\frac{\partial \boldsymbol{\rho}}{\partial x}(x,t),$$

  but in scheme $(C1)$ we are only upwinding the second one.

- The second scheme (C2)

$$\frac{d}{dt}\int_{C_i} \boldsymbol{\rho}(x,t)\,\mathrm{d}x + \mathbf{F}^{\rho}(x_{i+1/2},t,\boldsymbol{\rho}(x_{i+1/2},t)) - \mathbf{F}^{\rho}(x_{i-1/2},t,\boldsymbol{\rho}(x_{i-1/2},t))$$
$$- \int_{C_i} \mathbf{R}(x,t,\boldsymbol{\rho}(x,t))\,\mathrm{d}x = \int_{C_i} \mathbf{G}_5\big(x,t,\boldsymbol{\rho}(x,t)\big)\,\mathrm{d}x,$$

$$\mathbf{R}(x,t,\boldsymbol{\rho}) := \frac{\partial v}{\partial x}(x,t)\boldsymbol{\rho} \text{ and } \mathbf{G}_5(x,t,\boldsymbol{\rho}) := -\frac{\partial v}{\partial x}(x,t)\boldsymbol{\rho}.$$

- This scheme is fully independent of the one proposed for the Euler stage.
- It only considers the velocity computed at that stage.
- Consequently, the approximation of partial densities $\boldsymbol{\rho}(x_i, t_n)$ is quite different from the one used to approximate the total density $W_1(x_i, t_n)$.
- This fact provokes that the physical relation $W_1 = \sum_{k=1}^{N_e} \rho_k$ is not satisfied.
- Let us confirm this drawback by analysing a particular case.

- Assuming that $v^n_{i-1/2} > 0$ and $v^n_{i+1/2} > 0$ we will prove that the previous identity does not hold:

$$\begin{aligned}\sum_{k=1}^{N_e} \rho^{n+1}_{k,i} &= \sum_{k=1}^{N_e} \rho^n_{k,i} - \frac{\Delta t}{\Delta x}\left(v^n_i \sum_{k=1}^{N_e} \rho^n_{k,i} - v^n_{i-1} \sum_{k=1}^{N_e} \rho^n_{k,i-1} \right) \\ &= W^n_{1,i} - \frac{\Delta t}{\Delta x}\left(v^n_i W^n_{1,i} - v^n_{i-1} W^n_{1,i-1} \right).\end{aligned}$$

$$W^{n+1}_{1,i} = W^n_{1,i} - \frac{\Delta t}{\Delta x}\left(\eta^{Rn}_i - \eta^{Ln}_i \right),$$

$$\eta^{Ln}_i := \phi^W_1\left(x_{i-1}, x_i, t_n, \boldsymbol{W}^n_{i-1}, \boldsymbol{W}^n_i \right) + \Delta x \sum_{j=1}^{4} \Psi^L_{j,1}\left(x_{i-1}, x_i, t_n, \boldsymbol{W}^n_{i-1}, \boldsymbol{W}^n_i \right),$$

$$\eta^{Rn}_i := \phi^W_1\left(x_i, x_{i+1}, t_n, \mathbf{W}^n_i, \mathbf{W}^n_{i+1} \right) - \Delta x \sum_{j=1}^{4} \Psi^R_{j,1}\left(x_i, x_{i+1}, t_n, \mathbf{W}^n_i, \mathbf{W}^n_{i+1} \right).$$

USC UNIVERSIDADE DE SANTIAGO DE COMPOSTELA

Grupo de Investigación en Ingeniería Matemática

The gas composition stage. The third scheme (C3)

- This new scheme satisfies $W_1 = \sum_{k=1}^{N_e} \rho_k$ at time t_{n+1}, assuming that it is satisfied at time t_n.
- We follow the same procedure introduced in (C2) but we will couple the composition stage to the Euler stage by replacing the velocities in the numerical flux of the former with the ones obtained from η_i^{Ln} and η_i^{Rn}, used to compute $W_{1,i}^{n+1}$ in (E2).
- We define new numerical fluxes of the Q-scheme of van Leer:

$$\mathbf{\Phi}_L^{\rho}(x_{i-1}, x_i, t_n, \boldsymbol{\rho}_{i-1}^n, \boldsymbol{\rho}_i^n) := \frac{1}{2}\left(\tilde{v}_{L,i-1}^n \boldsymbol{\rho}_{i-1}^n + \tilde{v}_{L,i}^n \boldsymbol{\rho}_i^n\right) - \frac{1}{2}|\tilde{v}_{L,i-1/2}^n|(\boldsymbol{\rho}_i^n - \boldsymbol{\rho}_{i-1}^n),$$

$$\mathbf{\Phi}_R^{\rho}(x_i, x_{i+1}, t_n, \boldsymbol{\rho}_i^n, \boldsymbol{\rho}_{i+1}^n) := \frac{1}{2}\left(\tilde{v}_{R,i}^n \boldsymbol{\rho}_i^n + \tilde{v}_{R,i+1}^n \boldsymbol{\rho}_{i+1}^n\right) - \frac{1}{2}|\tilde{v}_{R,i+1/2}^n|(\boldsymbol{\rho}_{i+1}^n - \boldsymbol{\rho}_i^n),$$

- The new approximations of velocities are

$$
\begin{aligned}
\tilde{v}^n_{L,i-1} &:= \eta_i^{Ln} \frac{1}{W^n_{1,i-1}}, \quad \tilde{v}^n_{L,i} := \eta_i^{Ln} \frac{1}{W^n_{1,i}}, \\
\tilde{v}^n_{L,i-1/2} &:= \frac{1}{2}\left(\tilde{v}^n_{L,i-1} + \tilde{v}^n_{L,i}\right) = \eta_i^{Ln} \frac{1}{2}\left(\frac{1}{W^n_{1,i-1}} + \frac{1}{W^n_{1,i}}\right), \\
\tilde{v}^n_{R,i} &:= \eta_i^{Rn} \frac{1}{W^n_{1,i}}, \quad \tilde{v}^n_{R,i+1} := \eta_i^{Rn} \frac{1}{W^n_{1,i+1}}, \\
\tilde{v}^n_{R,i+1/2} &:= \frac{1}{2}\left(\tilde{v}^n_{R,i} + \tilde{v}^n_{R,i+1}\right) = \eta_i^{Rn} \frac{1}{2}\left(\frac{1}{W^n_{1,i}} + \frac{1}{W^n_{1,i+1}}\right)
\end{aligned}
$$

- Accordingly, the upwind discretization of the source term $\mathbf{G}_{5,i}^n$ corresponds to

$$\begin{aligned}
\boldsymbol{\Psi}_5^L(x_{i-1}, x_i, t_n, \boldsymbol{\rho}_{i-1}^n, \boldsymbol{\rho}_i^n) &= -\frac{1}{2}\left(\mathcal{I} + \frac{|\tilde{v}_{L,i-1/2}^n|}{\tilde{v}_{L,i-1/2}^n}\mathcal{I}\right)\mathbf{R}_i^{Ln}, \\
\boldsymbol{\Psi}_5^R(x_i, x_{i+1}, t_n, \boldsymbol{\rho}_i^n, \boldsymbol{\rho}_{i+1}^n) &= -\frac{1}{2}\left(\mathcal{I} - \frac{|\tilde{v}_{R,i+1/2}^n|}{\tilde{v}_{R,i+1/2}^n}\mathcal{I}\right)\mathbf{R}_i^{Rn},
\end{aligned}$$

where

$$\begin{aligned}
\mathbf{R}_i^{Ln} &= \frac{\tilde{v}_{L,i}^n - \tilde{v}_{L,i-1/2}^n}{\Delta x}\boldsymbol{\rho}_i^n + \frac{\tilde{v}_{L,i-1/2}^n - \tilde{v}_{L,i-1}^n}{\Delta x}\boldsymbol{\rho}_{i-1}^n, \\
\mathbf{R}_i^{Rn} &= \frac{\tilde{v}_{R,i+1}^n - \tilde{v}_{R,i+1/2}^n}{\Delta x}\boldsymbol{\rho}_{i+1}^n + \frac{\tilde{v}_{R,i+1/2}^n - \tilde{v}_{R,i}^n}{\Delta x}\boldsymbol{\rho}_i^n.
\end{aligned}$$

USC UNIVERSIDADE DE SANTIAGO DE COMPOSTELA

Grupo de Investigación en Ingeniería Matemática

- Then, after some algebra, we can rewrite this new scheme as

$$\frac{\boldsymbol{\rho}_i^{n+1}-\boldsymbol{\rho}_i^n}{\Delta t}+\frac{1}{\Delta x}\left(\boldsymbol{\varphi}_i^{Rn}(x_i,x_{i+1},t_n,\boldsymbol{\rho}_i^n,\boldsymbol{\rho}_{i+1}^n)-\boldsymbol{\varphi}_i^{Ln}(x_{i-1},x_i,t_n,\boldsymbol{\rho}_{i-1}^n,\boldsymbol{\rho}_i^n)\right)=\mathbf{0},$$

where the global numerical fluxes $\boldsymbol{\varphi}_i^{Ln}$ and $\boldsymbol{\varphi}_i^{Rn}$ are defined by

$$\boldsymbol{\varphi}_i^{Ln}(x_{i-1},x_i,t_n,\boldsymbol{\rho}_{i-1}^n,\boldsymbol{\rho}_i^n)=\begin{cases}\tilde{v}_{L,i-1}^n\boldsymbol{\rho}_{i-1}^n & \text{if} \quad \tilde{v}_{L,i-1/2}^n>0,\\ \tilde{v}_{L,i}^n\boldsymbol{\rho}_i^n & \text{if} \quad \tilde{v}_{L,i-1/2}^n\leq 0,\end{cases}$$

$$\boldsymbol{\varphi}_i^{Rn}(x_i,x_{i+1},t_n,\boldsymbol{\rho}_i^n,\boldsymbol{\rho}_{i+1}^n)=\begin{cases}\tilde{v}_{R,i}^n\boldsymbol{\rho}_i^n & \text{if} \quad \tilde{v}_{R,i+1/2}^n>0,\\ \tilde{v}_{R,i+1}^n\boldsymbol{\rho}_{i+1}^n & \text{if} \quad \tilde{v}_{R,i+1/2}^n\leq 0.\end{cases}$$

- This scheme preserves the positivity of partial densities ρ_k if the CFL condition is satisfied.

USC UNIVERSIDADE DE SANTIAGO DE COMPOSTELA

Grupo de Investigación en Ingeniería Matemática

This new scheme satisfies the suitable property, $W_1^{n+1} = \sum_{k=1}^{N_e} \rho_k^{n+1}$, assuming that $W_{1,i}^n = \sum_{k=1}^{N_e} \rho_{k,i}^n$, $\forall i$.

- Let us denote $\varphi_{k,i}^{Ln} := \varphi_k^{Ln}(x_{i-1}, x_i, t_n, \boldsymbol{\rho}_{i-1}^n, \boldsymbol{\rho}_i^n)$ and $\varphi_{k,i}^{Rn} := \varphi_k^{Rn}(x_i, x_{i+1}, t_n, \boldsymbol{\rho}_i^n, \boldsymbol{\rho}_{i+1}^n)$.

$$\sum_{k=1}^{N_e} \varphi_{k,i}^{Ln} = \left\{ \begin{array}{ll} \tilde{v}_{L,i-1}^n \displaystyle\sum_{k=1}^{N_e} \rho_{k,i-1}^n = \eta_i^{Ln} \frac{1}{W_{1,i-1}^n} \sum_{k=1}^{N_e} \rho_{k,i-1}^n & \text{if} \quad \tilde{v}_{L,i-1/2}^n > 0 \\ \tilde{v}_{L,i}^n \displaystyle\sum_{k=1}^{N_e} \rho_{k,i}^n = \eta_i^{Ln} \frac{1}{W_{1,i}^n} \sum_{k=1}^{N_e} \rho_{k,i}^n & \text{if} \quad \tilde{v}_{L,i-1/2}^n \leq 0 \end{array} \right\} = \eta_i^{Ln},$$

and also $\sum_{k=1}^{N_e} \varphi_{k,i}^{Rn} = \eta_i^{Rn}$. Then,

$$\sum_{k=1}^{N_e} \rho_{k,i}^{n+1} = \sum_{k=1}^{N_e} \rho_{k,i}^n - \frac{\Delta t}{\Delta x} \left(\sum_{k=1}^{N_e} \varphi_{k,i}^{Rn} - \sum_{k=1}^{N_e} \varphi_{k,i}^{Ln} \right) = W_{1,i}^{n+1}.$$

USC UNIVERSIDADE DE SANTIAGO DE COMPOSTELA

mat+i Grupo de Investigación en Ingeniería Matemática

Imposing boundary conditions

- In academic tests designed to analyze the order of accuracy of the numerical discretizations, it is a usual practice to impose the values of the exact solution at the boundary nodes.
- This practice avoids that the accuracy of the method can be affected by the treatment of boundary conditions.
- From the mathematical point of view, it is like considering Dirichlet boundary conditions.

Test 1

- The initial condition consists in a static situation ($v = 0$) with spatially constant $R\theta = K$.

$$\rho(x) = \frac{p(x)}{R(x)\theta(x)} = \frac{p(x)}{K}$$

$$\rho(x) = \rho(0)\exp\left(-\frac{g}{K}\left(h(x) - h(0)\right)\right).$$

$$\theta(x) = \begin{cases} \theta_L & \text{if} \quad x < \frac{\mathcal{L}}{2}, \\ \theta_R & \text{if} \quad x > \frac{\mathcal{L}}{2}, \end{cases}, \quad Y_k(x) = \begin{cases} Y_{kL} & \text{if} \quad x < \frac{\mathcal{L}}{2}, \\ Y_{kR} & \text{if} \quad x > \frac{\mathcal{L}}{2}, \end{cases}, \; k = 1, \cdots, 5,$$

where species are methane, ethane, propane, butane and nitrogen, respectively.

USC UNIVERSIDADE DE SANTIAGO DE COMPOSTELA

Grupo de Investigación en Ingeniería Matemática

Test 1

Y_{1L}	Y_{1R}	Y_{2L}	Y_{2R}	Y_{3L}	Y_{3R}	Y_{4L}	Y_{4R}	Y_{5L}	Y_{5R}
0.95	0.70	0.03	0.05	0.015	0.10	0.025	0.15	00025	0

Table: Data for Test 1 (I)

θ_L (C)	θ_R(C)	$R\theta$	$h(x)$ (m)	$\mathcal{L}$ (m)
4.965142	63.434338	140329	$200 \sin\left(\frac{4\pi x}{\mathcal{L}}\right)$	10000

Table: Data for Test 1 (II)

Test 1

- The initial condition consists in a static situation ($v = 0$) with spatially constant $R\theta$.

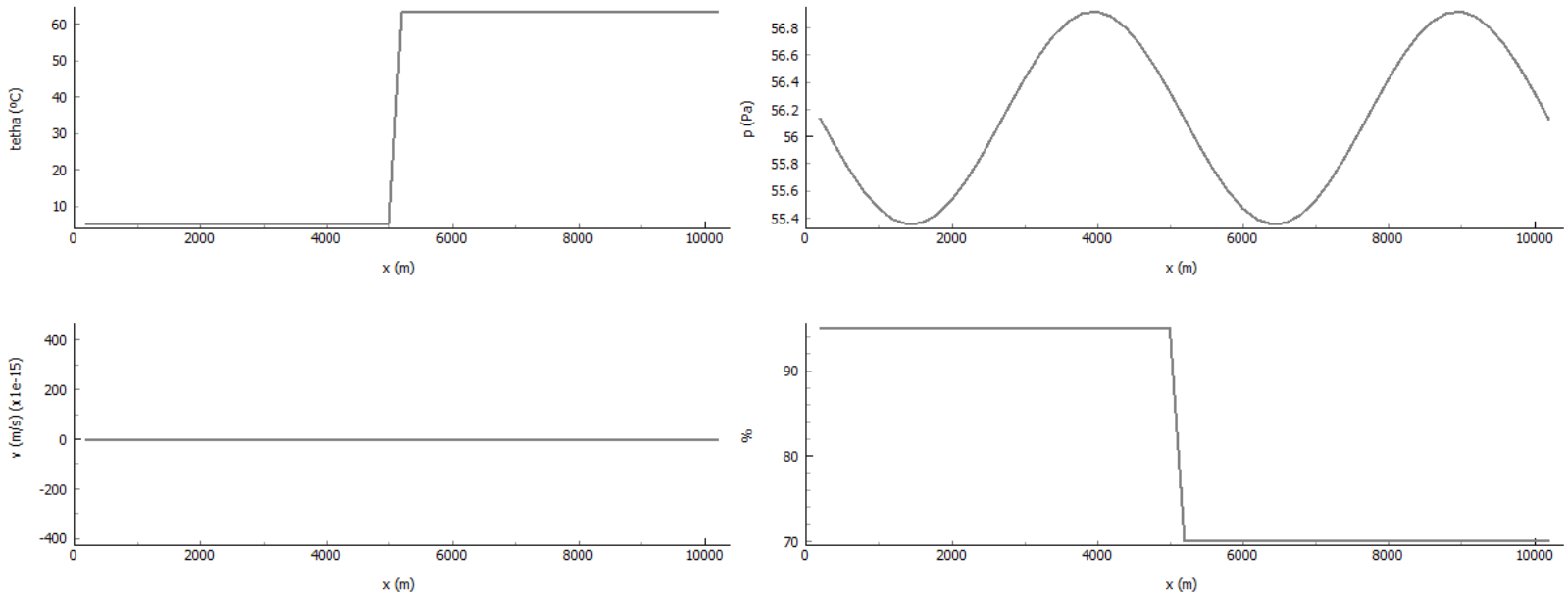

Test 1. Numerical results with (E1)+(C3)

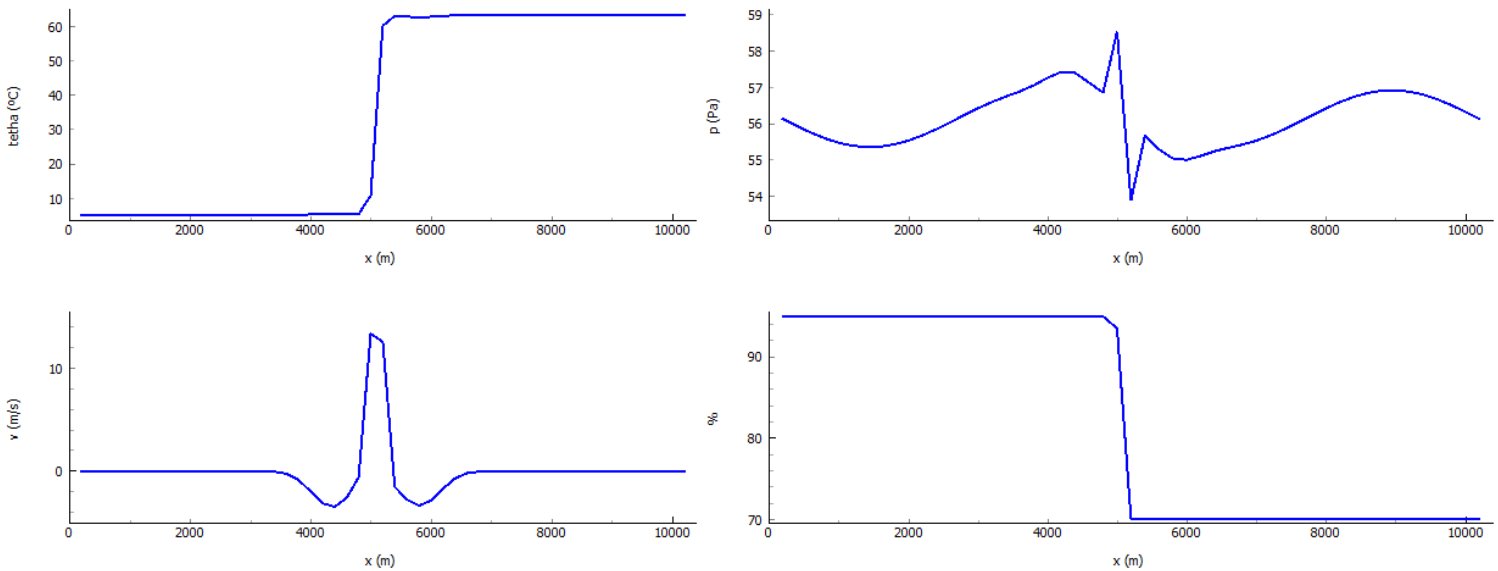

Figure: Numerical results with scheme (E1)+(C3). Above: temperature (left) and pressure (right). Below: velocity (left) and mass fraction $100\,Y_1$ (right). $t = 2s$.

The velocity is fully wrong: roughly speaking it oscillates between $v_{min} \simeq -4.6$ m/s and $v_{Max} \simeq 15$ m/s while the exact velocity is null.
The computed pressure is also wrong near $x = \frac{\mathcal{L}}{2}$.

Test 1. Numerical results with (E1)+(C3)

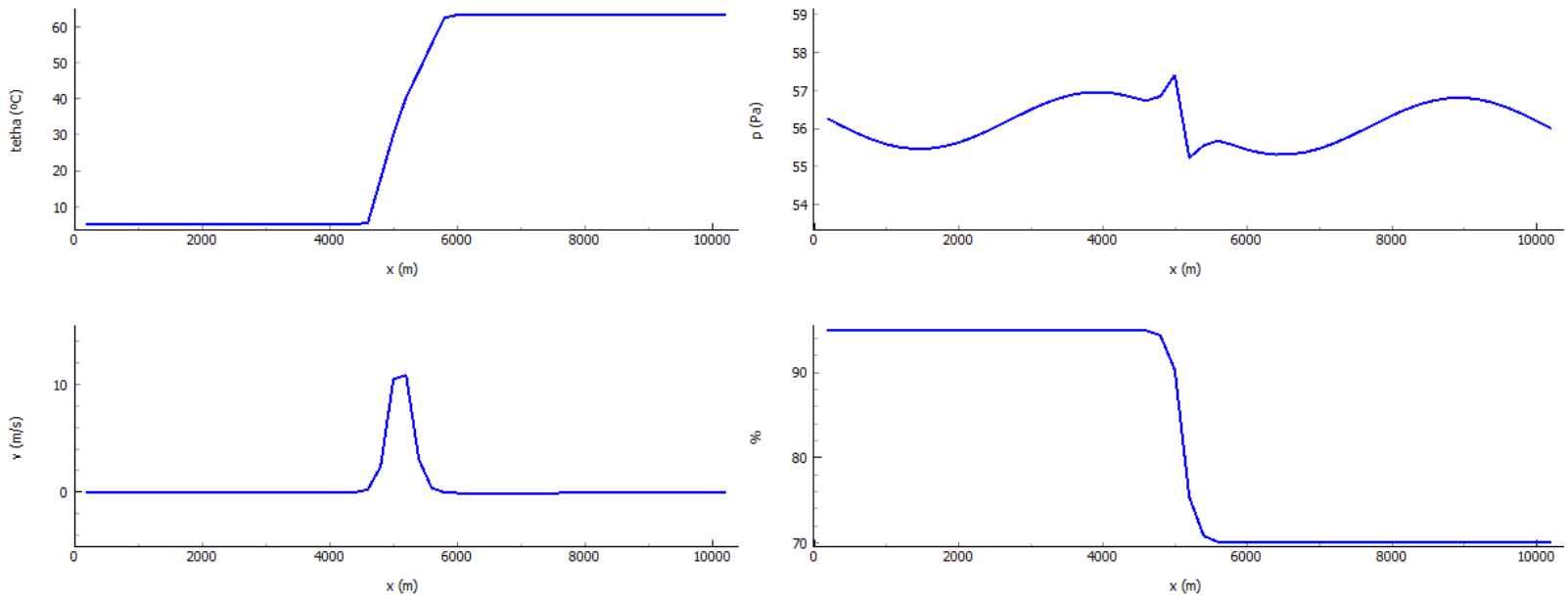

Figure: Numerical results with scheme (E1)+(C3). Above: temperature (left) and pressure (right). Below: velocity (left) and mass fraction $100\,Y_1$ (right). $t = 200s$.

Test 1. Numerical results with (E2)+(C2)

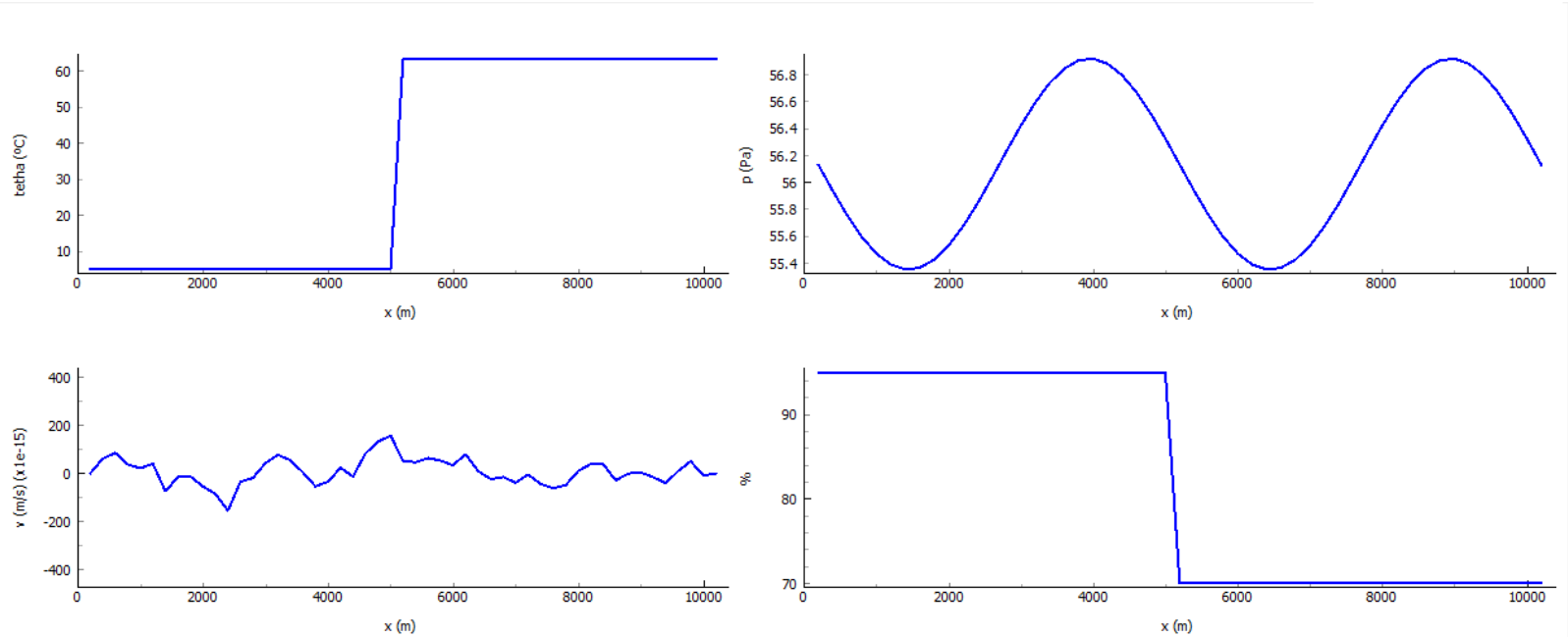

Figure: Numerical results with (E2)+(C2). Above: temperature (left) and pressure (right). Below: velocity (left) and mass fraction $100\,Y_1$ (right). $t = 2s$ (notice that the scale of velocities has to be multiplied by 10^{-15}).

The numerical results are in good agreement with the exact solution.

Test 1. Numerical results with (E2)+(C2)

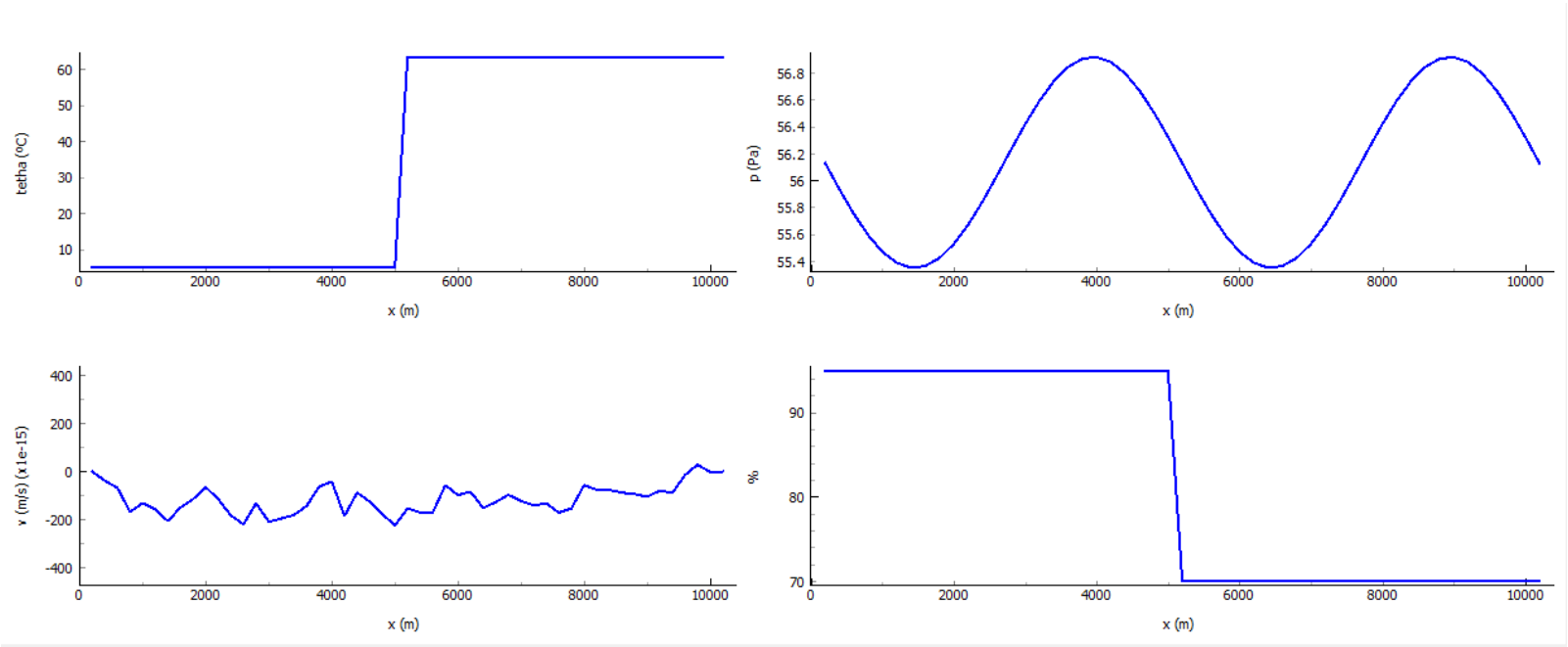

Figure: Numerical results with (E2)+(C2). Above: temperature (left) and pressure (right). Below: velocity (left) and mass fraction $100\,Y_1$ (right). $t = 200s$ (notice that the scale of velocities has to be multiplied by 10^{-15}).

Test 1. Numerical results with (E2)+(C3)

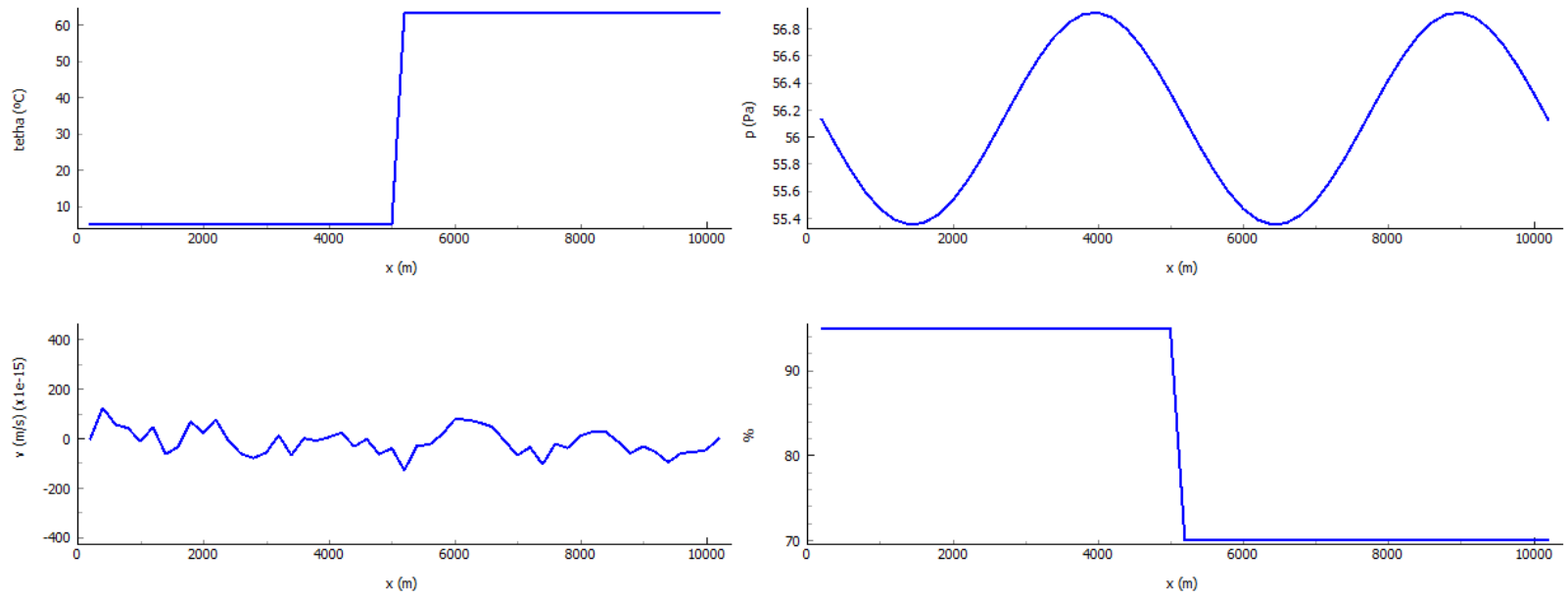

Figure: Numerical results with (E2)+(C3). Above: temperature (left) and pressure (right). Below: velocity (left) and mass fraction $100\,Y_1$ (right). $t = 2s$ (notice that the scale of velocities has to be multiplied by 10^{-15}).

The numerical results are in good agreement with the exact solution.

Test 1. Numerical results with (E2)+(C3)

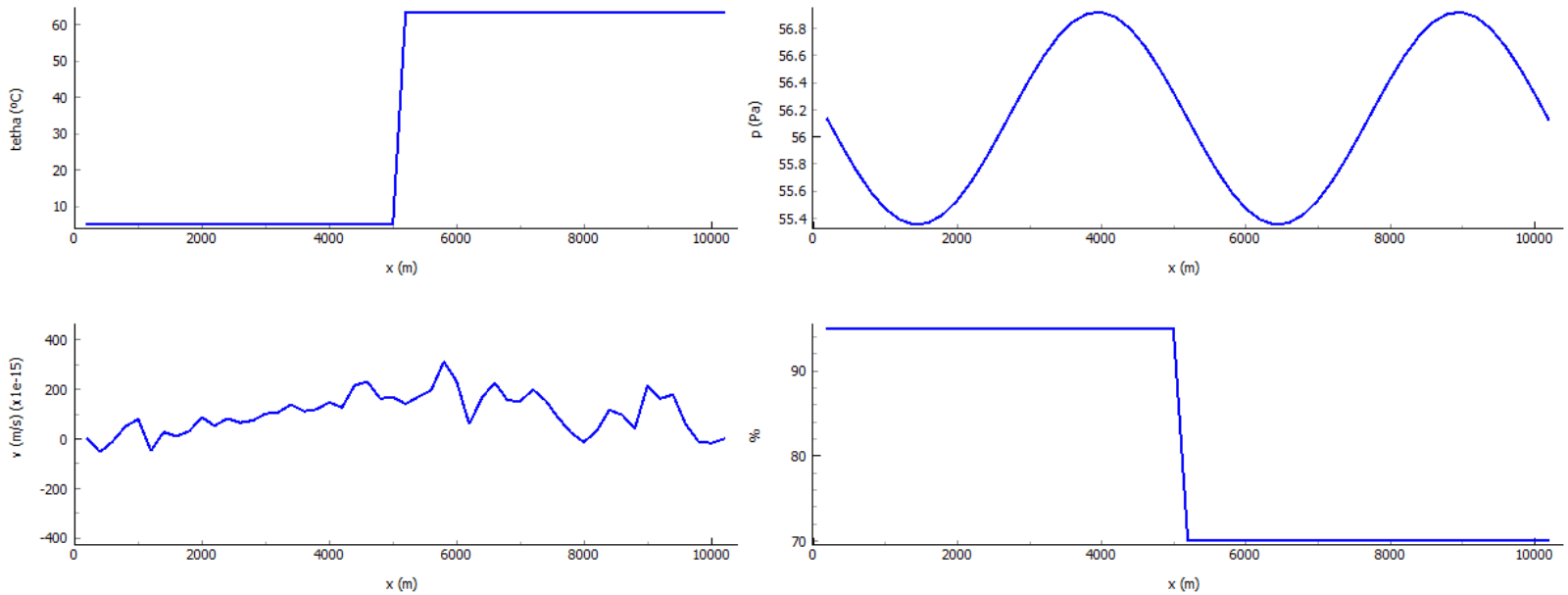

Figure: Numerical results with (E2)+(C3). Above: temperature (left) and pressure (right). Below: velocity (left) and mass fraction $100\,Y_1$ (right). $t = 200s$ (notice that the scale of velocities has to be multiplied by 10^{-15}).

Test 1

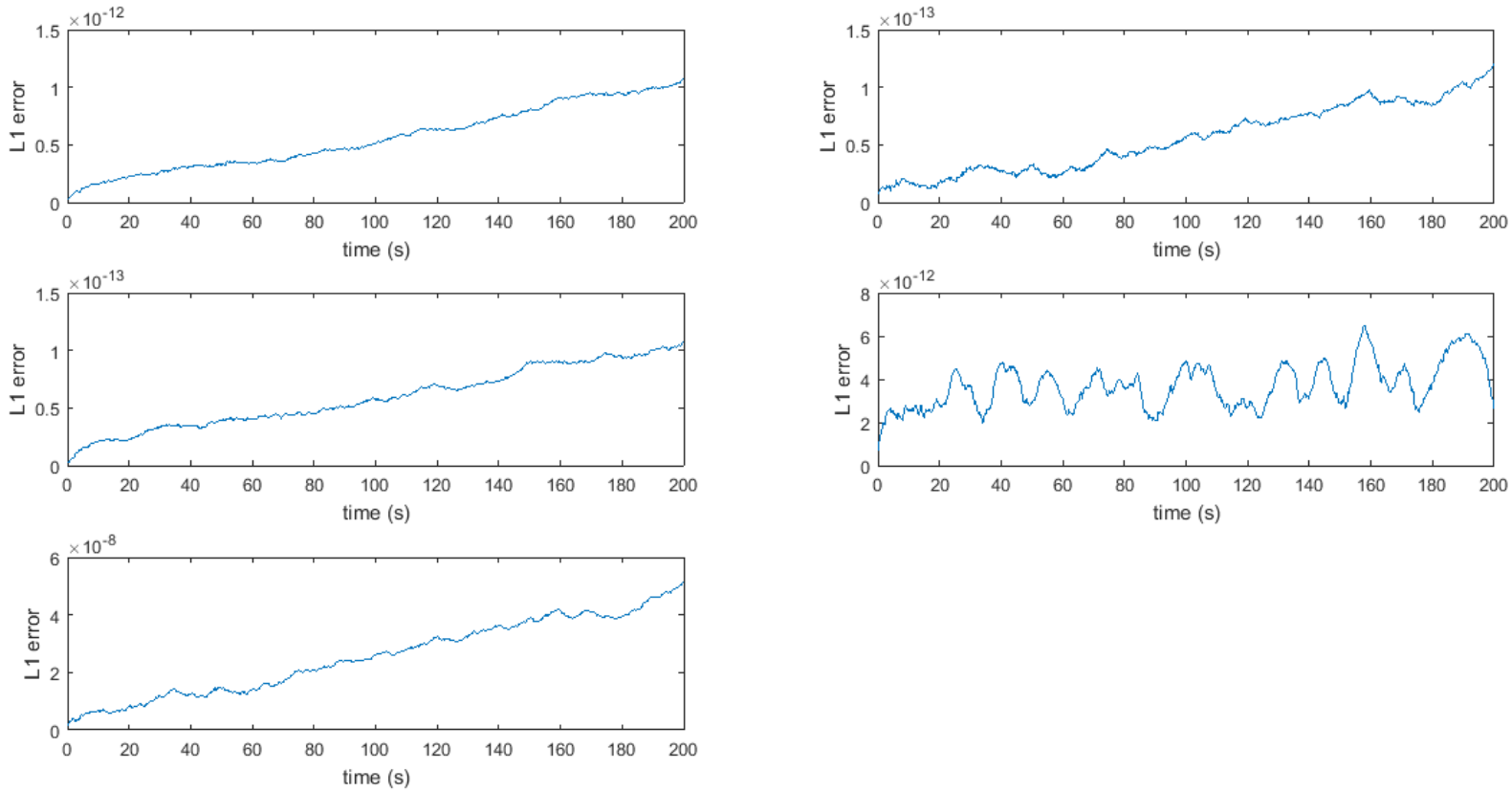

Figure: Test 1. $L1$-error evolution in time with scheme (E2)+(C3). Top: temperature (left) and pressure (right). Middle: density (left) and mass flux (right). Bottom: partial density ρ_1 (left). $t = 200s$.

Test 1. Numerical results with (E2)+(C4)

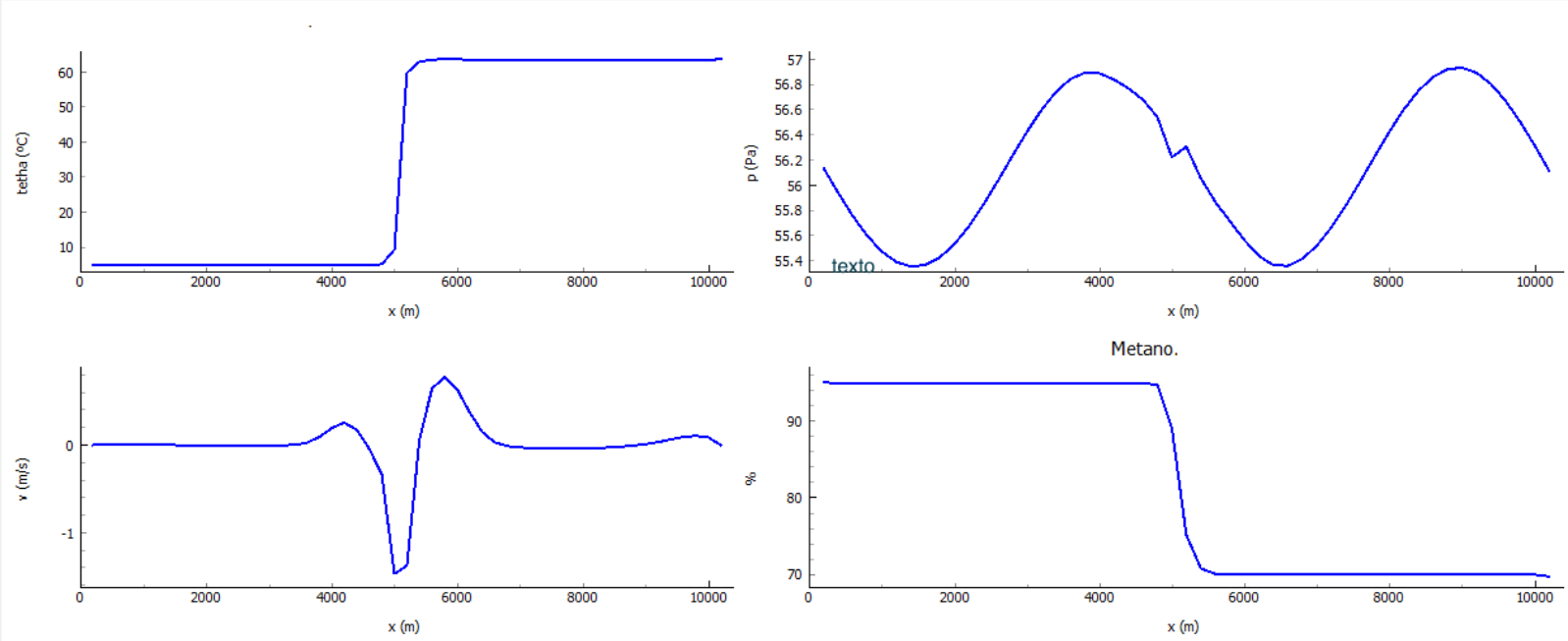

Figure: Numerical results with (E2)+(C4). Above: temperature (left) and pressure (right). Below: velocity (left) and mass fraction $100\,Y_1$ (right). $t = 2s$ (notice that the scale of velocities has to be multiplied by 10^{-15}).

For this scheme the results are not in good agreement with the exact solution.

Test 1. Numerical results with (E2)+(C4)

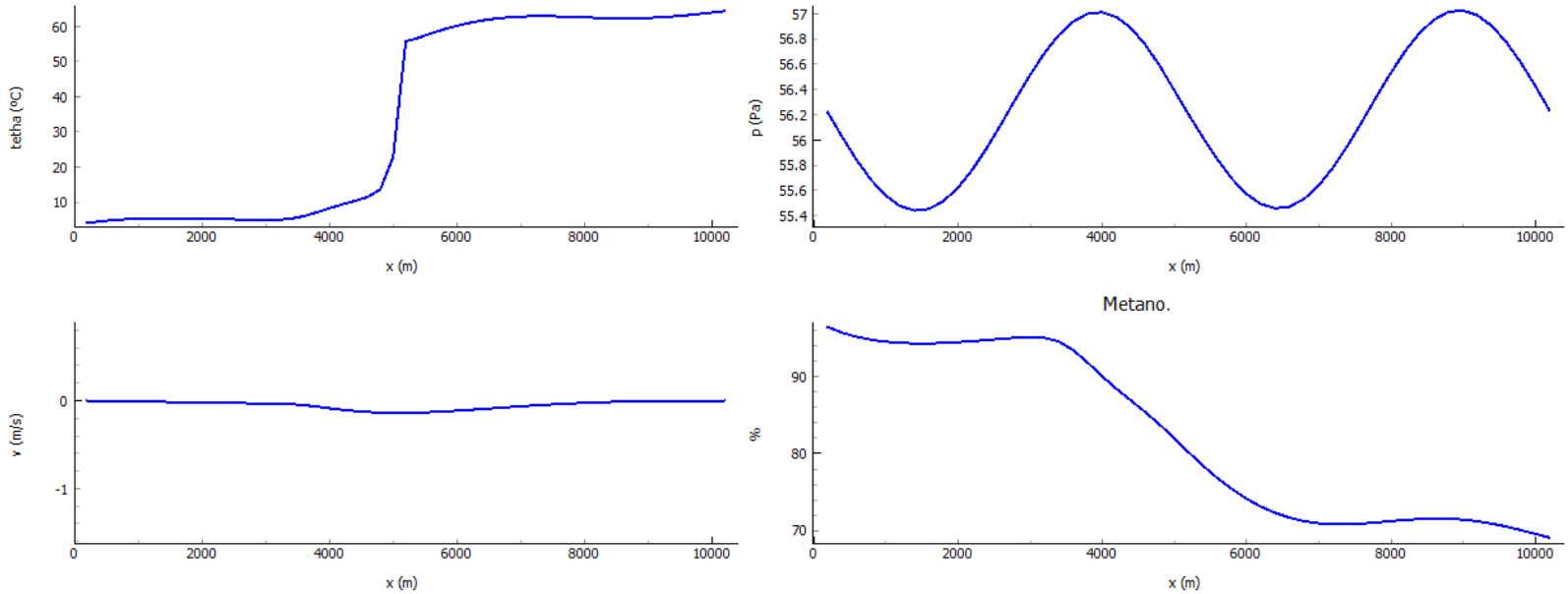

Figure: Numerical results with (E2)+(C4). Above: temperature (left) and pressure (right). Below: velocity (left) and mass fraction $100\,Y_1$ (right). $t = 200s$ (notice that the scale of velocities has to be multiplied by 10^{-15}).

For this scheme the results are not in good agreement with the exact solution.

Test 2.

- This case concerns a non-static situation ($v = v_c \neq 0$). We look for a steady solution for ρ and v such that

$$\rho(x,t) = \rho_c, \quad v(x,t) = v_c, \quad \theta(x)R(x) = K, \quad \forall x \in (0, \mathcal{L}).$$

  where ρ_c, v_c and K are constants.
- We assume that $h'(x) = 0$, and $\mathbf{G}_1$ and $\mathbf{G}_3$ are null at the Euler stage.
- Then, it is easy to check that the total energy E is the solution of a transport equation with constant velocity v_c.
- Moreover, if we assume that ρ_c, v_c are constant, then mass fractions $Y_k, k = 1, \cdots, N_e$ are also solution of the same linear transport equation.

Test 2.

Y_{1L}	Y_{1R}	Y_{2L}	Y_{2R}	Y_{3L}	Y_{3R}	Y_{4L}	Y_{4R}	Y_{5L}	Y_{5R}
0.70	0.95	0.05	0.03	0.10	0.015	0.15	0.0025	0	0.0025

Table: Data for Test 2 (I).

θ_L (C)	θ_R (C)	$K = R\theta$	$h(x)$ (m)	$\mathcal{L}$ (m)	ρ_c (kg/m^3)	v_c (m/s)
63.434338	4.965142	140329	0	10000	40	2

Table: Data for Test 2 (II).

Test 2

- Initial condition

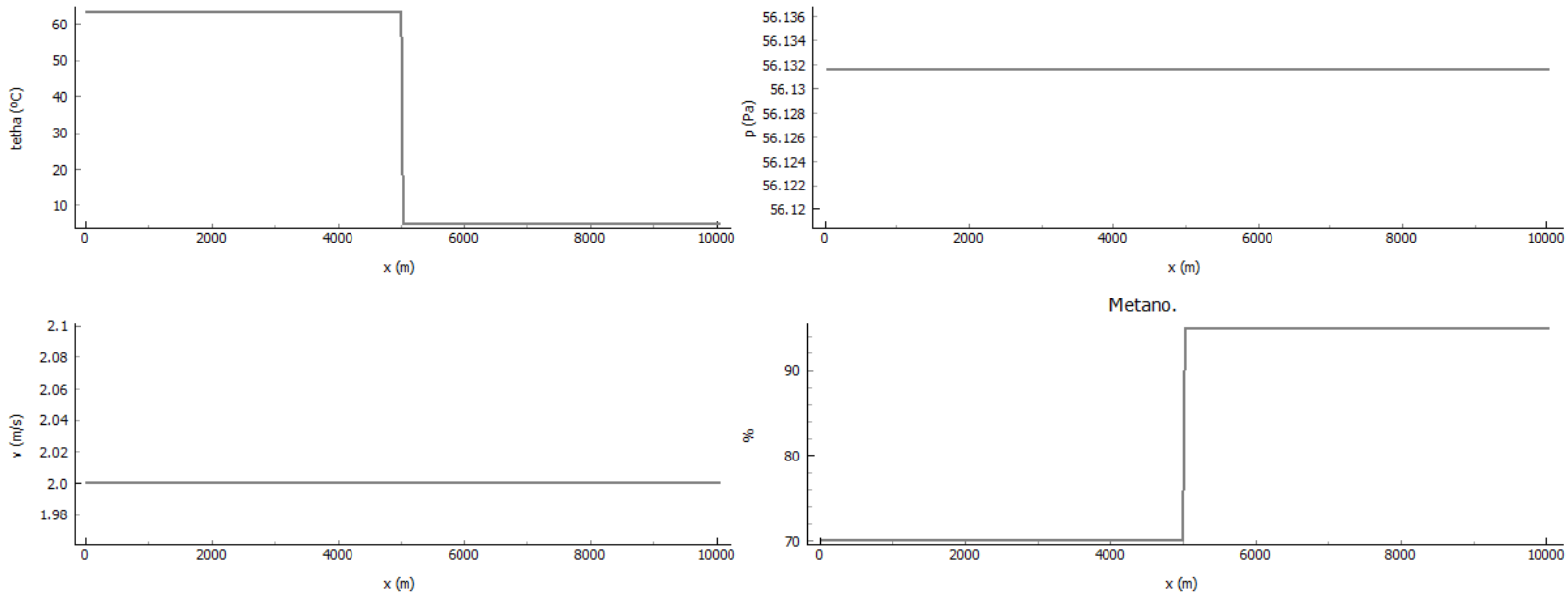

Test 2. Numerical results with (E2)+(C2) and (E2)+(C3)

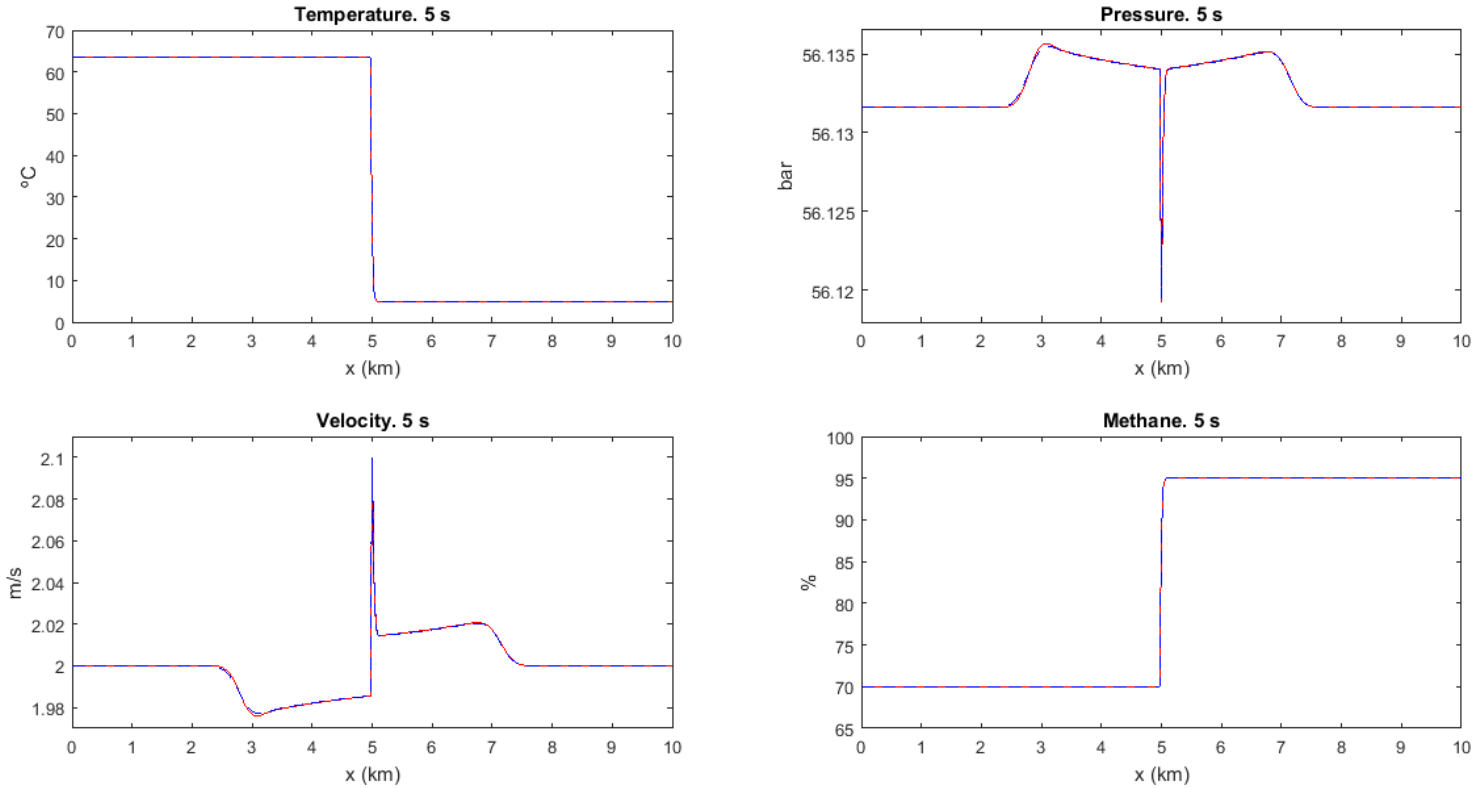

Figure: Numerical solutions with scheme (E2)+(C2) (blue), and with scheme (E2)+(C3) (red). Above: temperature (left) and pressure (right). Below: velocity (left) and mass fraction $100\,Y_1$ (right). $t = 5s$.

Test 2. Numerical results with (E2)+(C2) and (E2)+(C3)

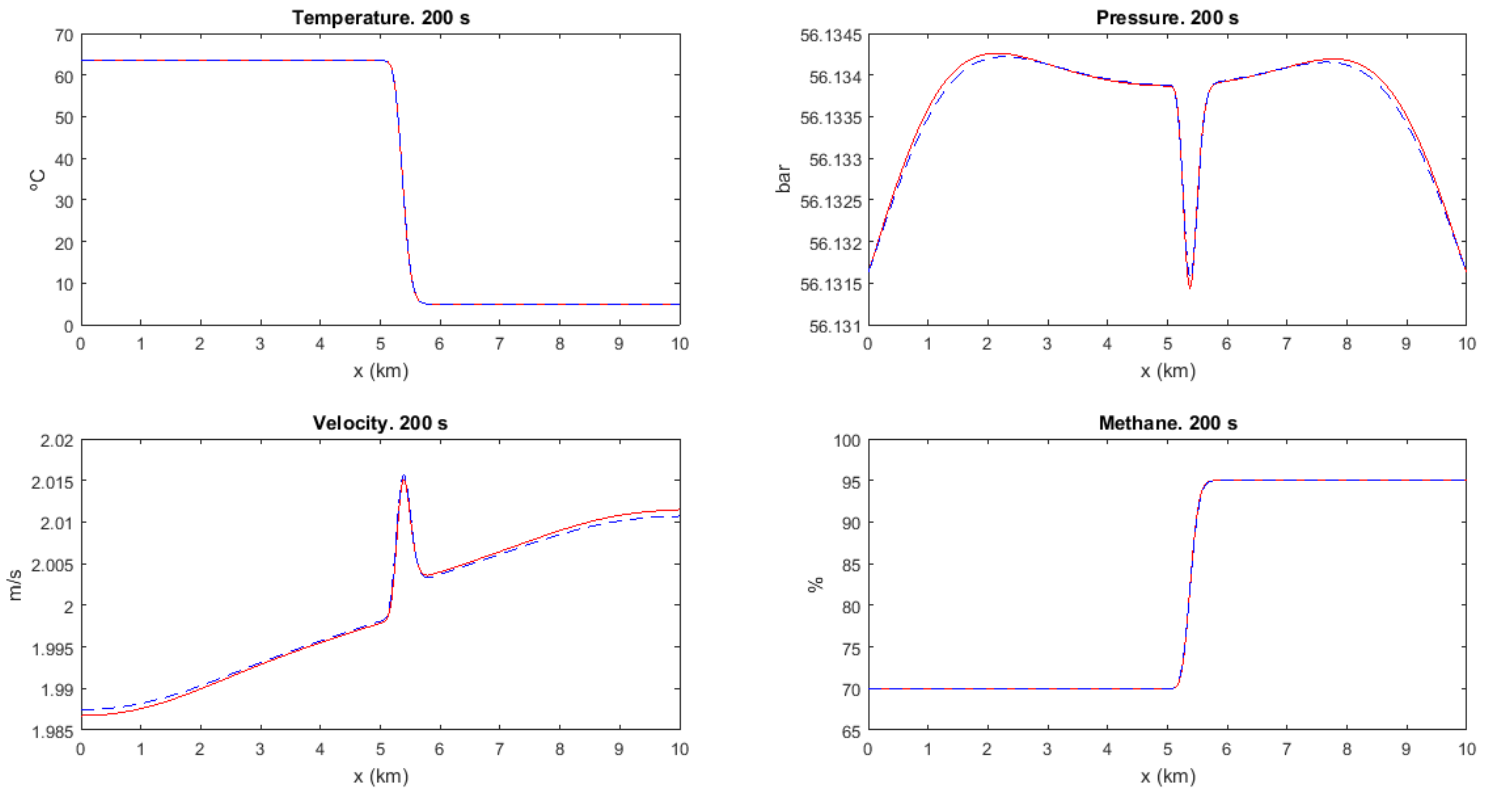

Figure: Numerical solutions with scheme (E2)+(C2) (blue), and with scheme (E2)+(C3) (red). Above: temperature (left) and pressure (right). Below: velocity (left) and mass fraction $100\,Y_1$ (right). $t = 200s$.

Gas network simulation

- The ultimate goal of the methodology proposed in this talk is the prediction of the physical variables involved in real gas transportation networks.
- In order to check if this is made accurately, we present a test involving real data.
- The network, depicted in next Figure, consists of 11 nodes, joined by 10 pipes.

Real gas network

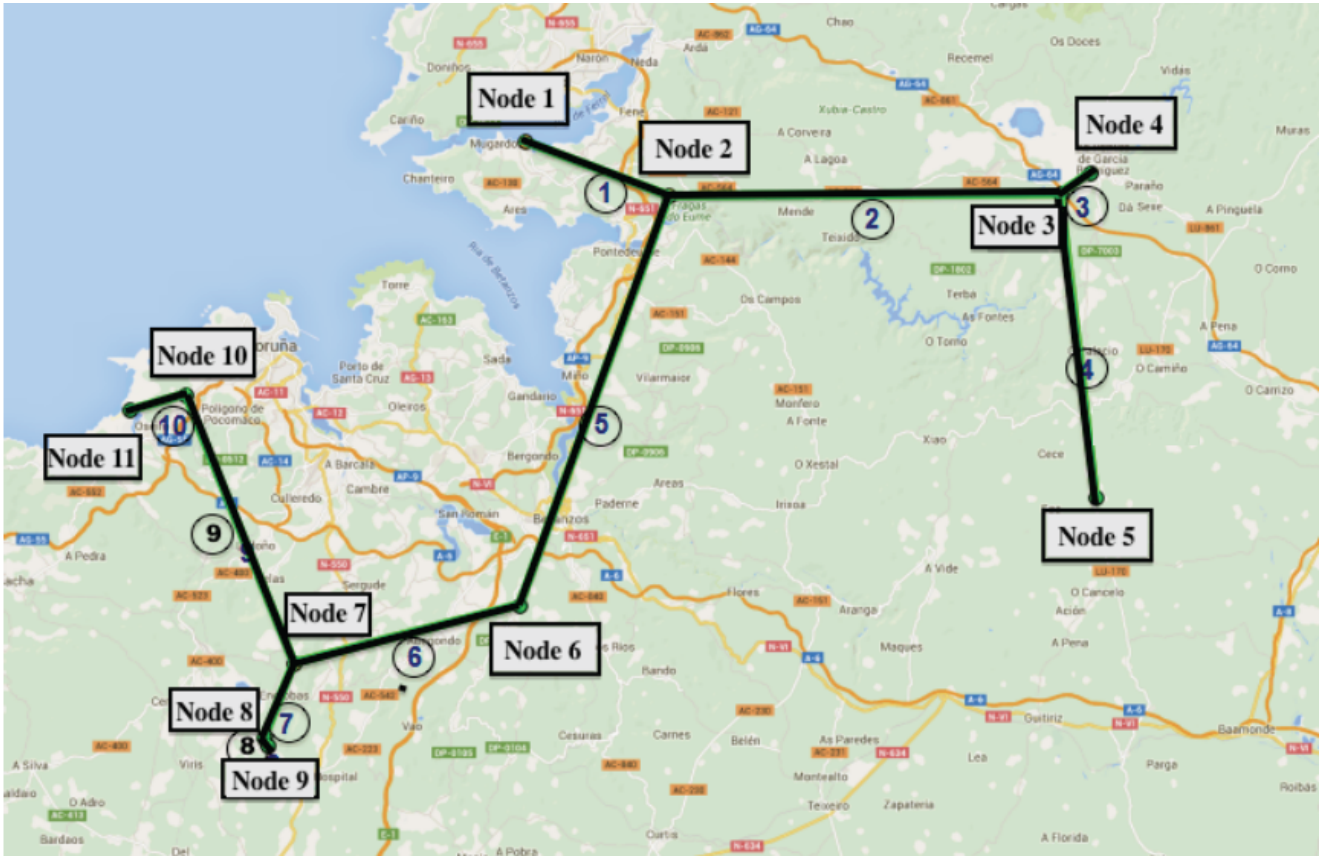

Figure: Real gas network, with node (rectangle) and edge (circle) identifications. (Galicia. Spain).

Topography is quite irregular

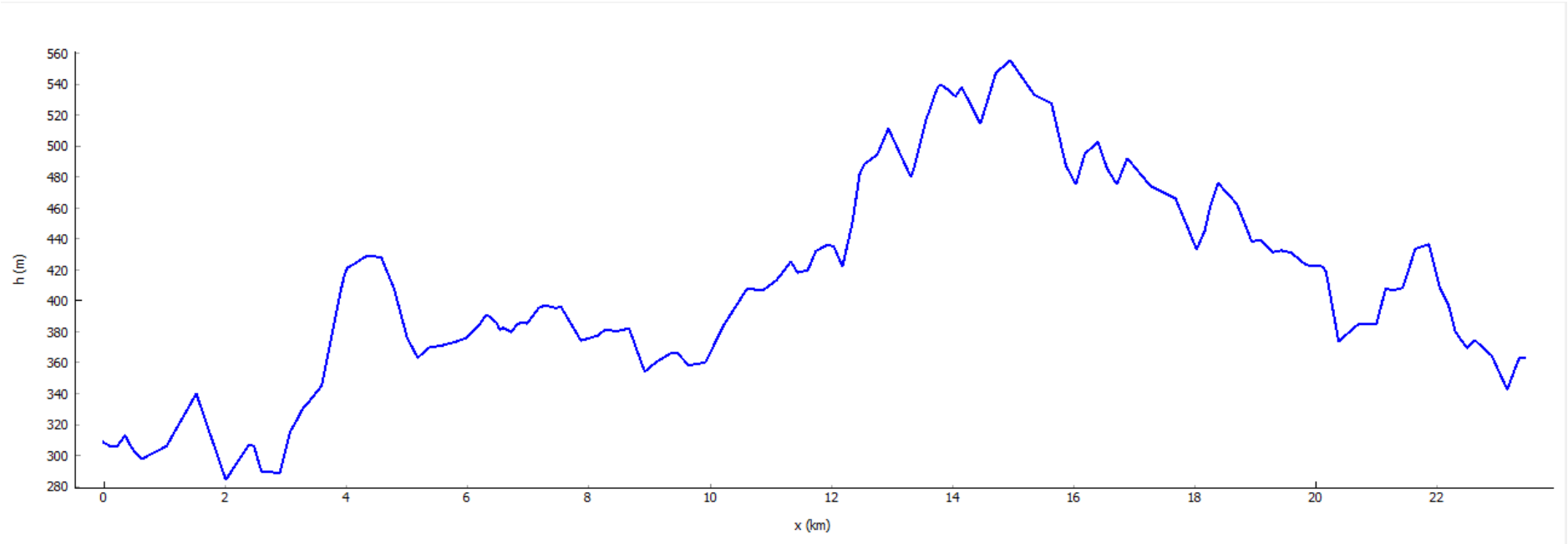

Figure: Test 4. Height profile along pipe number 4.

Test 3, real case.

- We present a test involving real data.
- We show the results obtained with schemes (E2)+(C2) and (E2)+(C3) along edge number 2.
- The variable height profile along this pipe is shown in previous figure.
- We select a real case with methane constant composition along the edge ($100\,Y_1 = 81.372634114$) and show the numerical results obtained with the above mentioned schemes.
- At $t = 20$ s the velocity along the pipe is not constant and, furthermore it changes sign. For this magnitude both schemes gives similar results for schemes (E2)+(C2) and (E2)+(C3).
- However, regarding methane mass fraction these schemes give different solutions.

USC UNIVERSIDADE DE SANTIAGO DE COMPOSTELA

Grupo de Investigación en Ingeniería Matemática

Test 3, real case. Numerical results with (E2)+(C2)

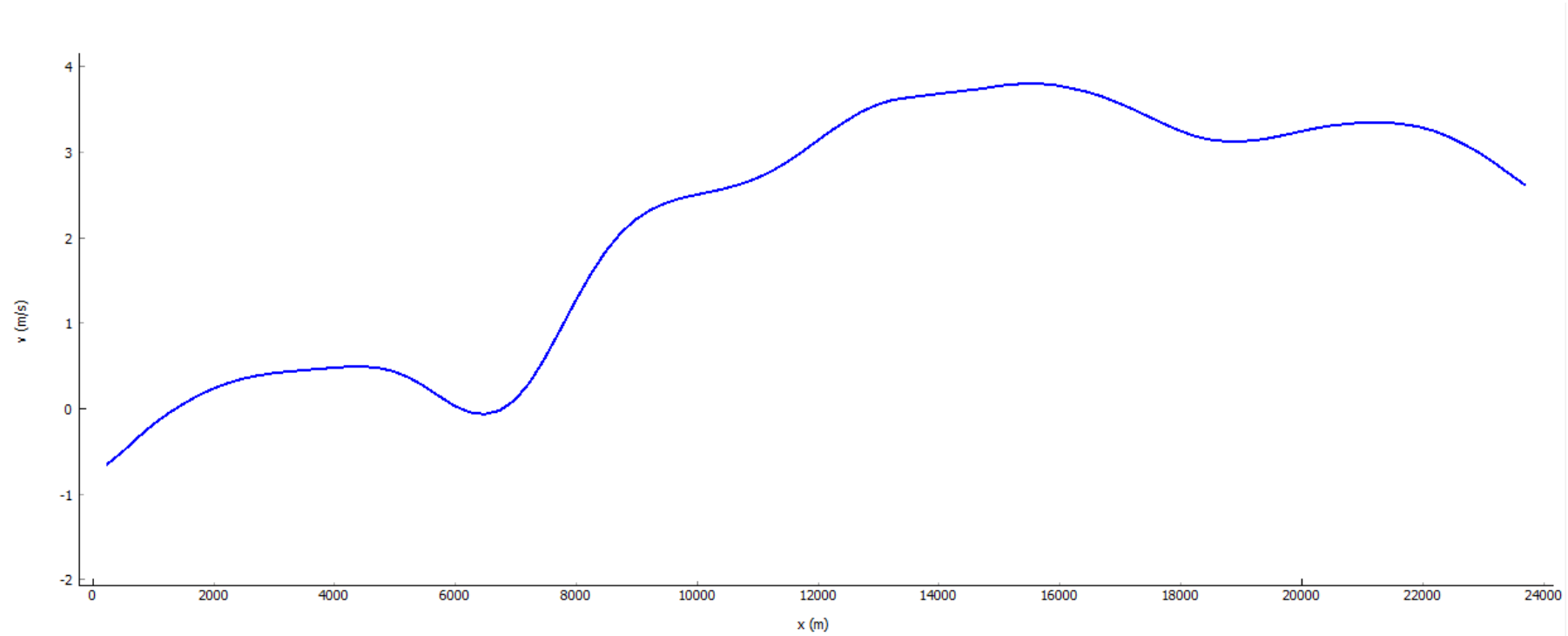

Figure: Velocity along pipe number 2 with scheme (E2)+(C2) . $t = 20$ s.

Test 3, real case. Numerical results with (E2)+(C3)

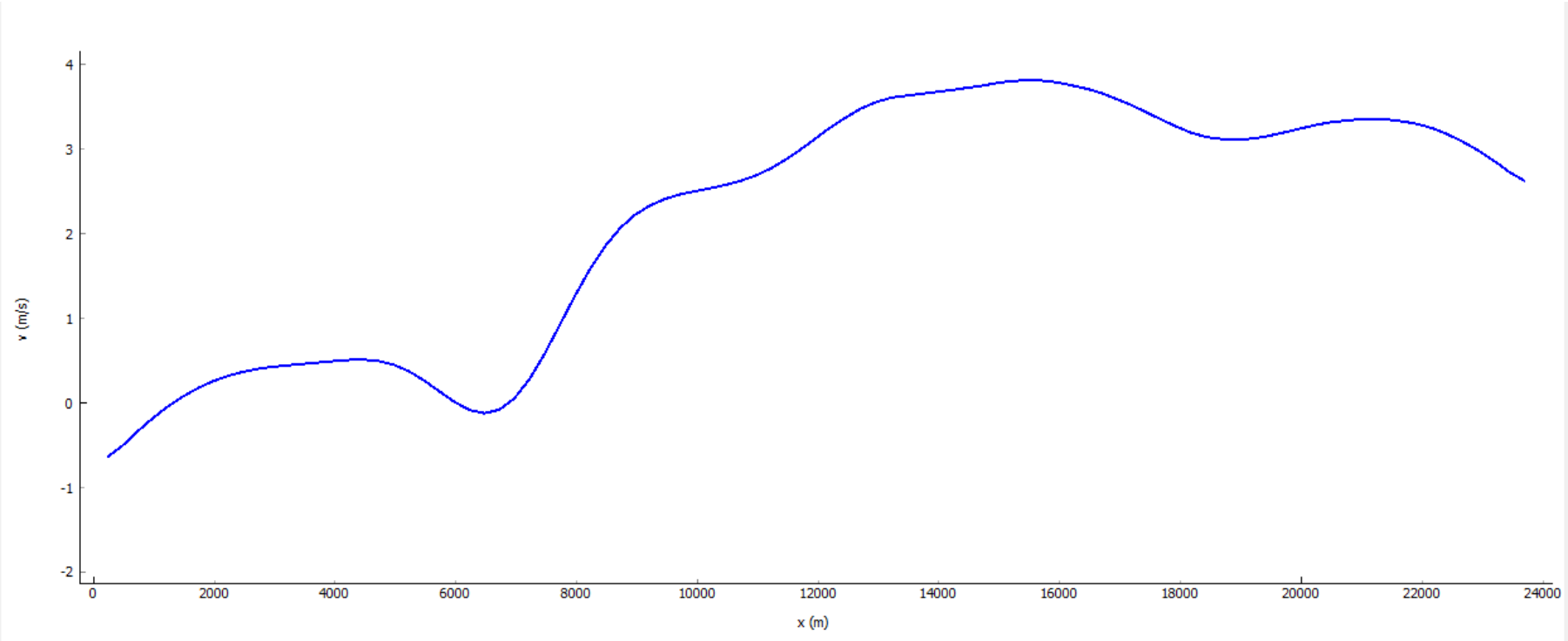

Figure: Velocity along pipe number 2 with scheme (E2)+(C3) . $t = 20$ s.

Test 3, real case. Numerical results with (E2)+(C2)

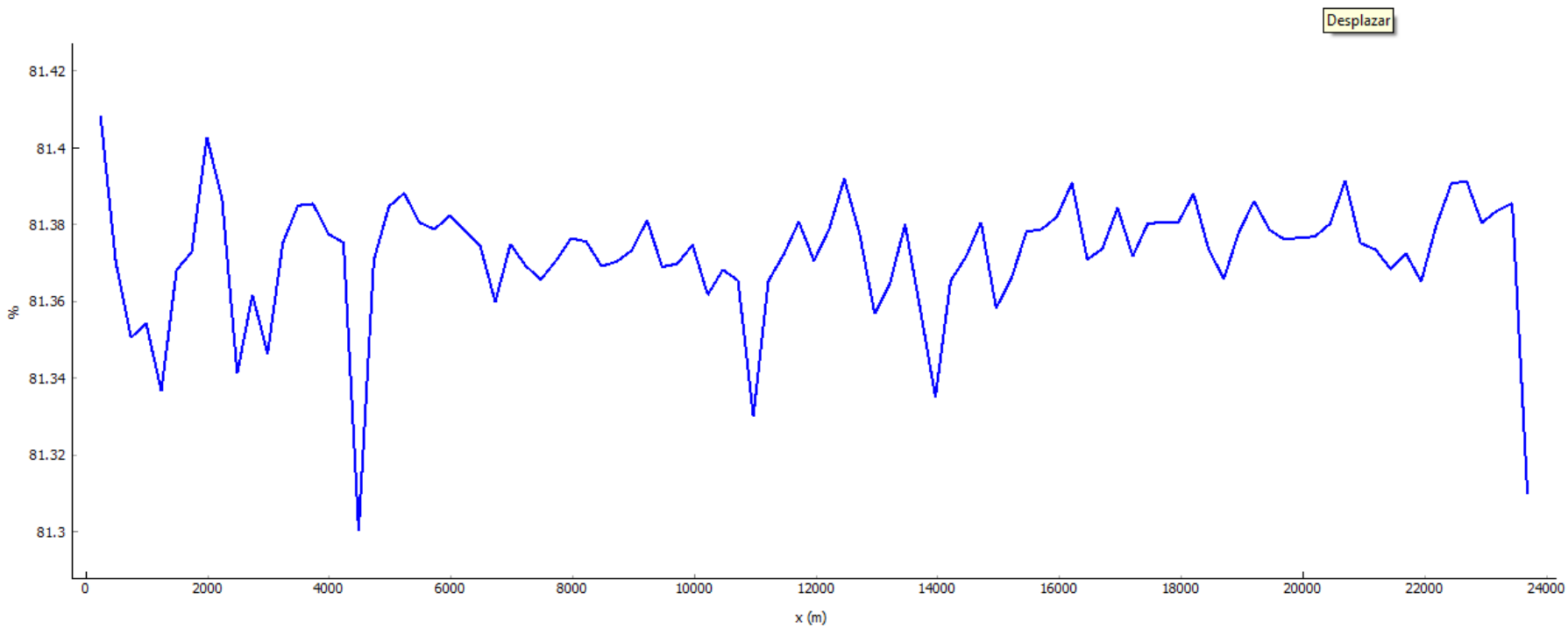

Figure: Mass fraction $100\,Y_1$ along pipe number 2 with scheme (E2)+(C2) . $t = 20$ s.

Test 3, real case. Numerical results with (E2)+(C3)

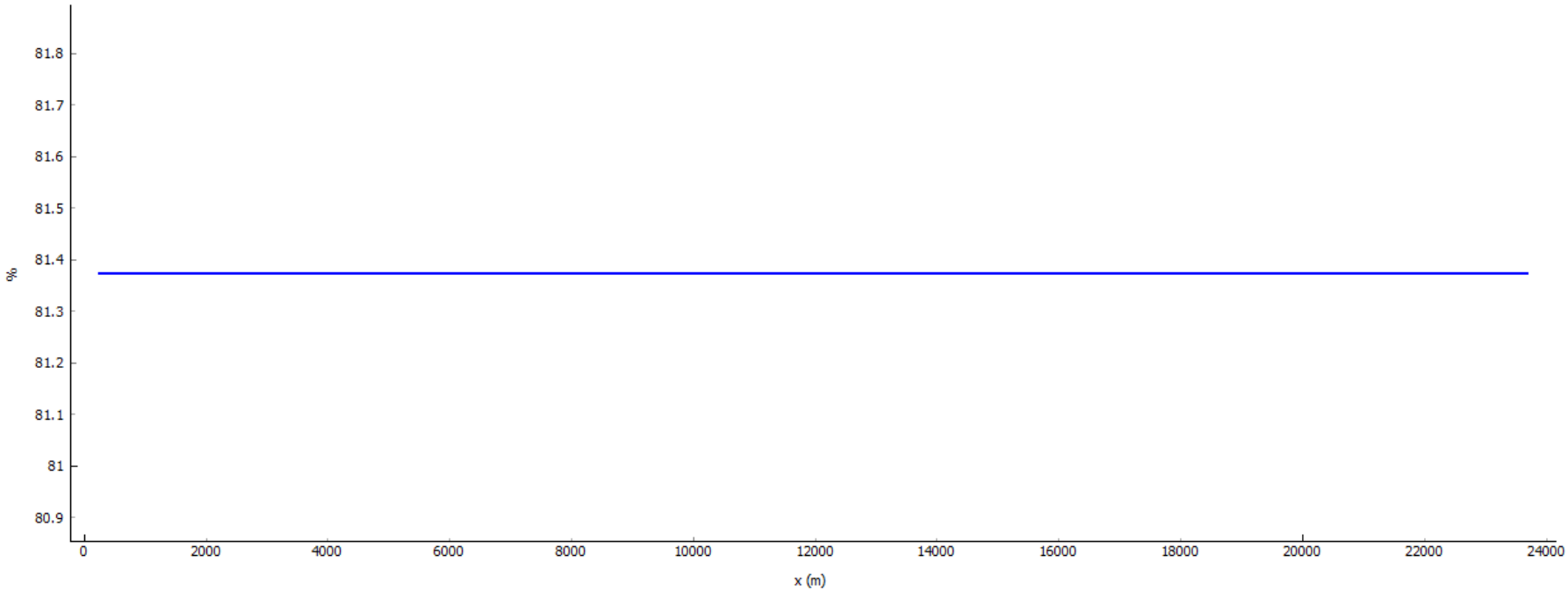

Figure: Mass fraction $100\,Y_1$ along pipe number 2 with scheme (E2)+(C3) . $t = 20$ s.

Test 4. Gas network simulation

- Node 01A represents the Reganosa's regasification plant. This is the only gas inlet into the whole network: the rest of the nodes are outlets.
- The main gas outlet is located at node I-013 which is a terminal node of the network where an outflow boundary condition is considered; the consumptions of the rest of the nodes are very small in comparison with this one.
- In order to take into account the consumption at the interior nodes we introduce an edge for each and impose an outflow boundary condition at its terminal node.

USC UNIVERSIDADE DE SANTIAGO DE COMPOSTELA

Grupo de Investigación en Ingeniería Matemática

Test 4. Data: Initial conditions, height profile

- Initial condition is based on the values of pressure, mass flow and temperature at the nodes, that are interpolated over the edges.
- In addition, we have the height profile of every gaseoduct.
- The total time period for which we make this test is 172800 s, in other words, 2 days.

Test 4. Numerical results: mass flow rate

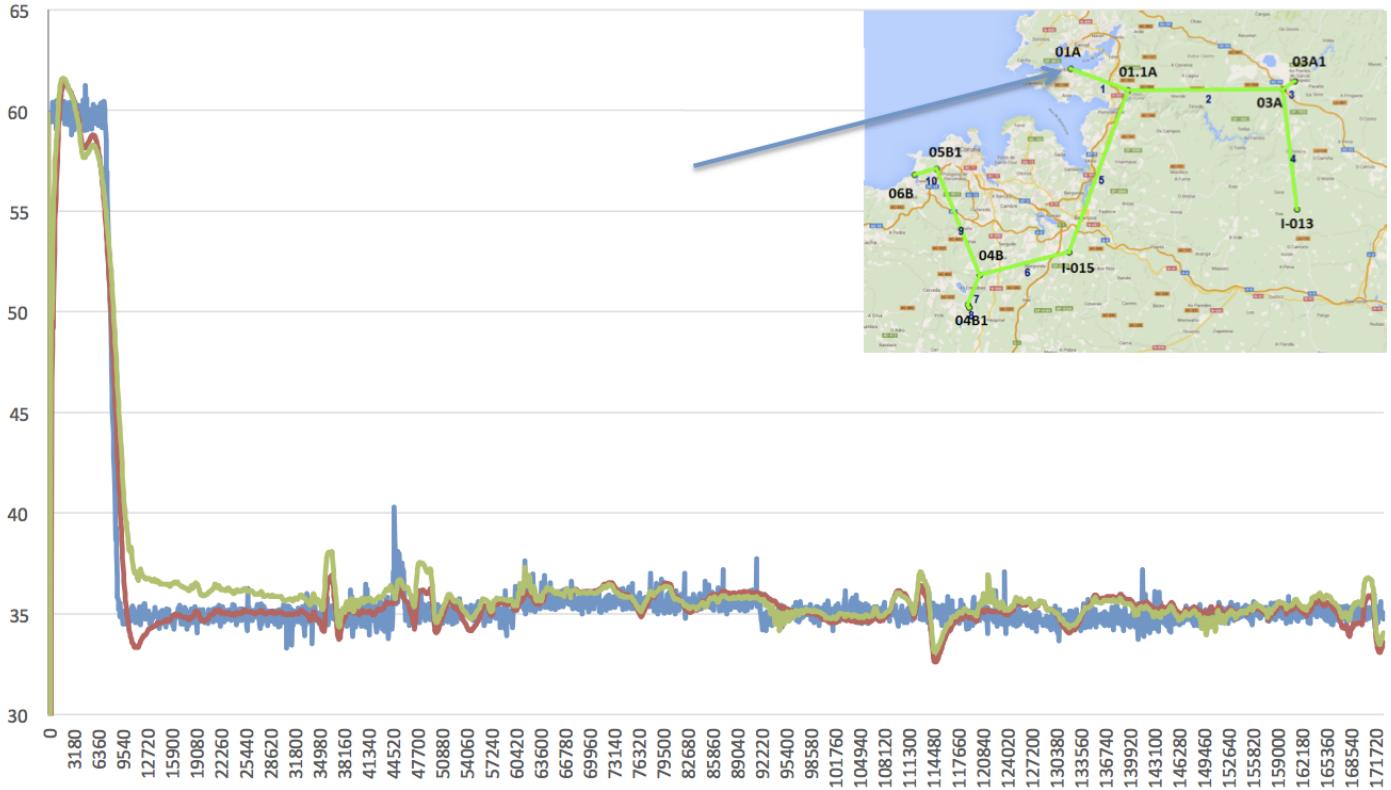

Figure: Mass flow at node **01A**. Blue: real measurement. Red: computed with a homogeneous gas composition model. Green: computed with a variable gas composition model.

xTest 4. Numerical results: Pressure

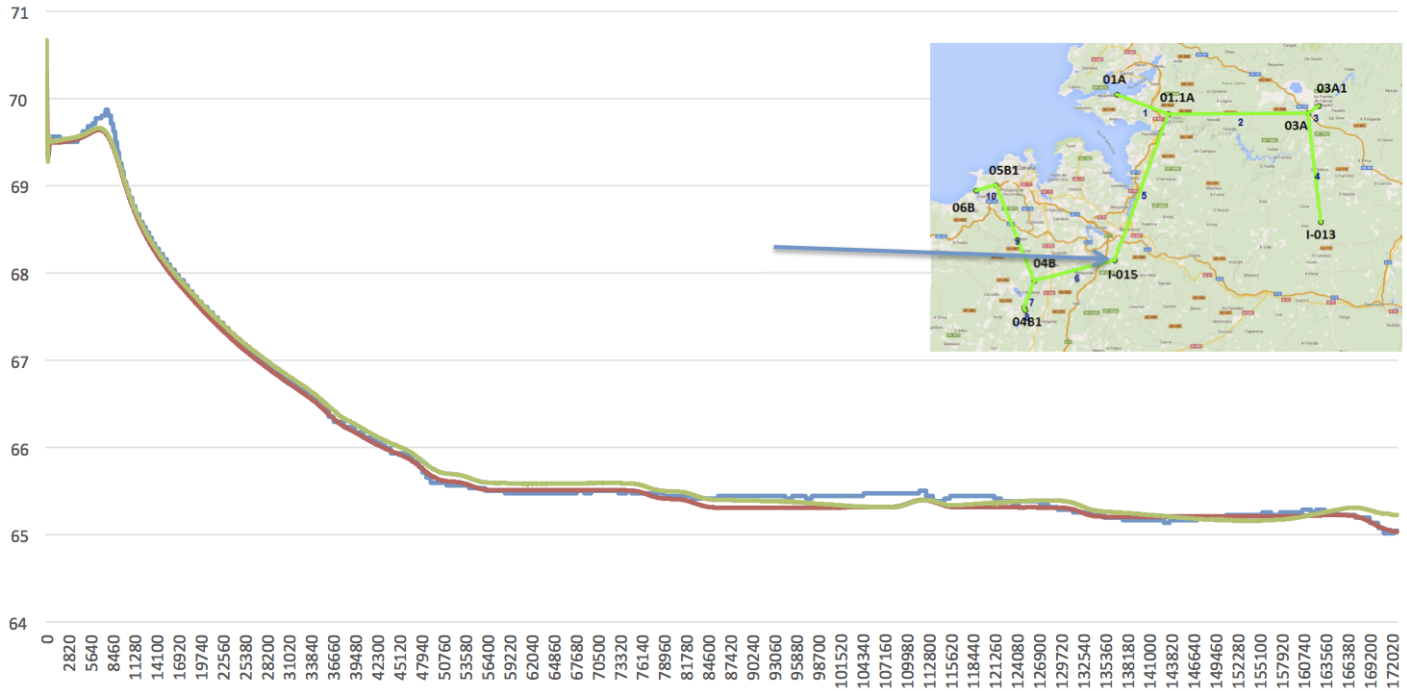

Figure: Pressure at node **I-015**. Blue: real measurement. Red: computed with a homogeneous gas composition model. Green: computed with a variable gas composition model.

Test 4. Numerical results: Pressure

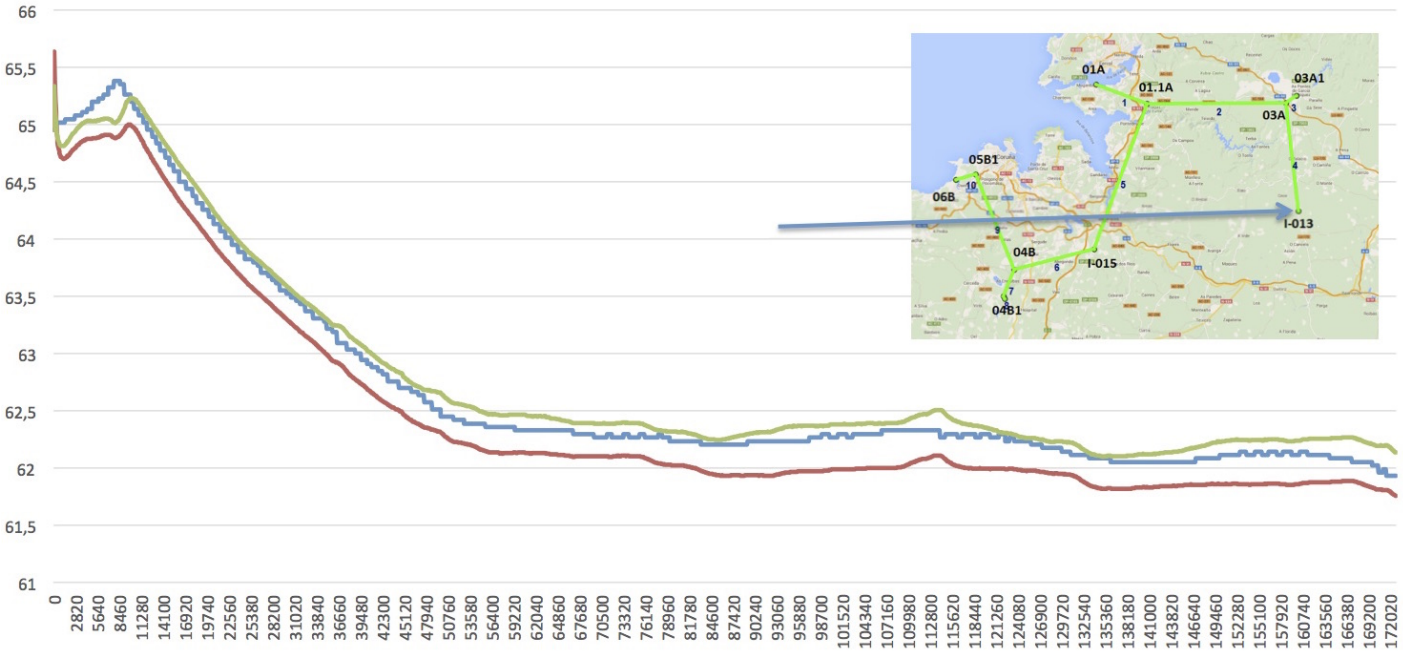

Figure: Pressure at node **I-013**. Blue: real measurement. Red: computed with a homogeneous gas composition model. Green: computed with a variable gas composition model.

Test 4.Numerical results: Pressure

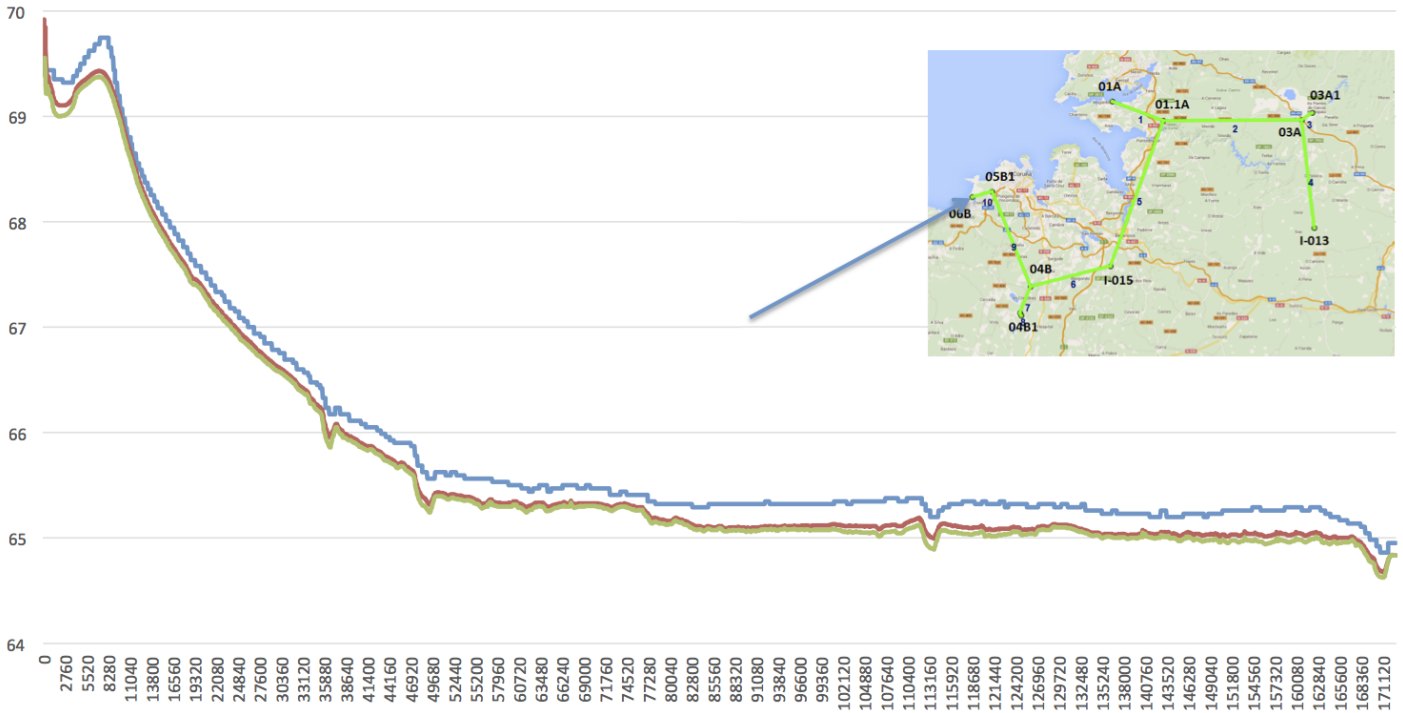

Figure: Pressure at node **06B**. Blue: real measurement. Red: computed with a homogeneous gas composition model. Green: computed with a variable gas composition model.

Test 5.Numerical results with (E2)+(C3)

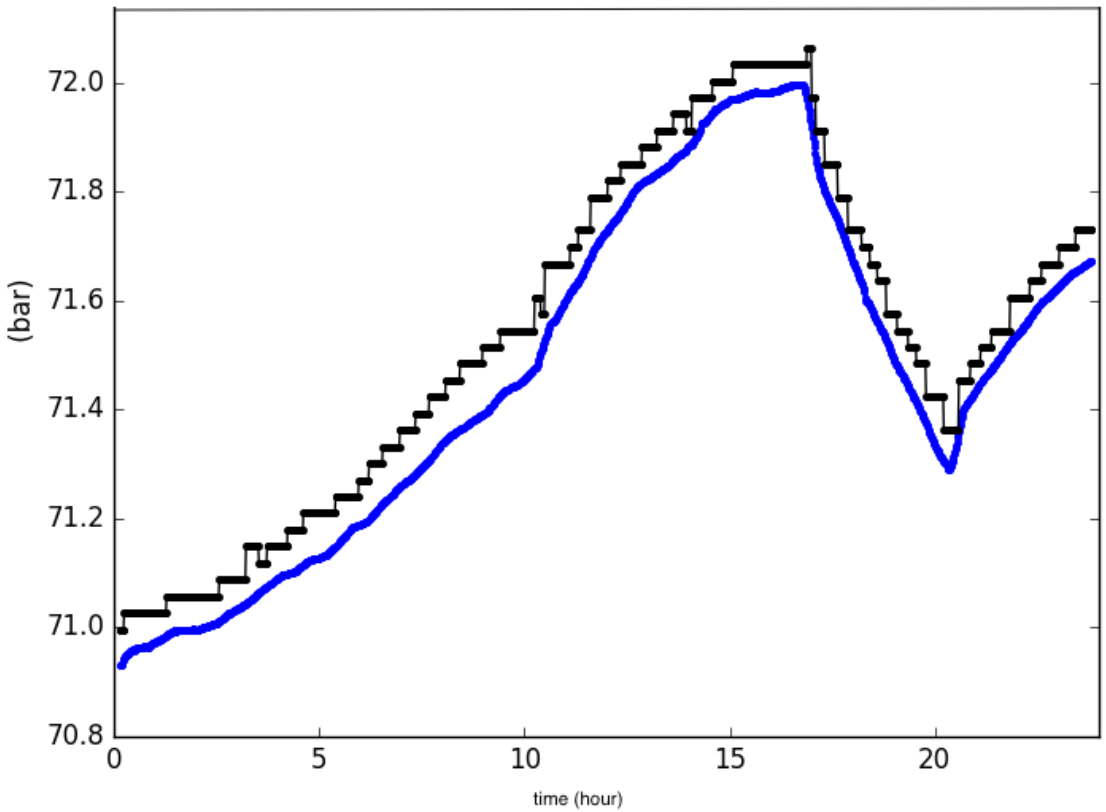

Figure: Pressure at node 5 for one day. Black: real measurement. Blue: computed.

USC UNIVERSIDADE DE SANTIAGO DE COMPOSTELA

mat+i Grupo de Investigación en Ingeniería Matemática

Test 5.Numerical results with (E2)+(C3)

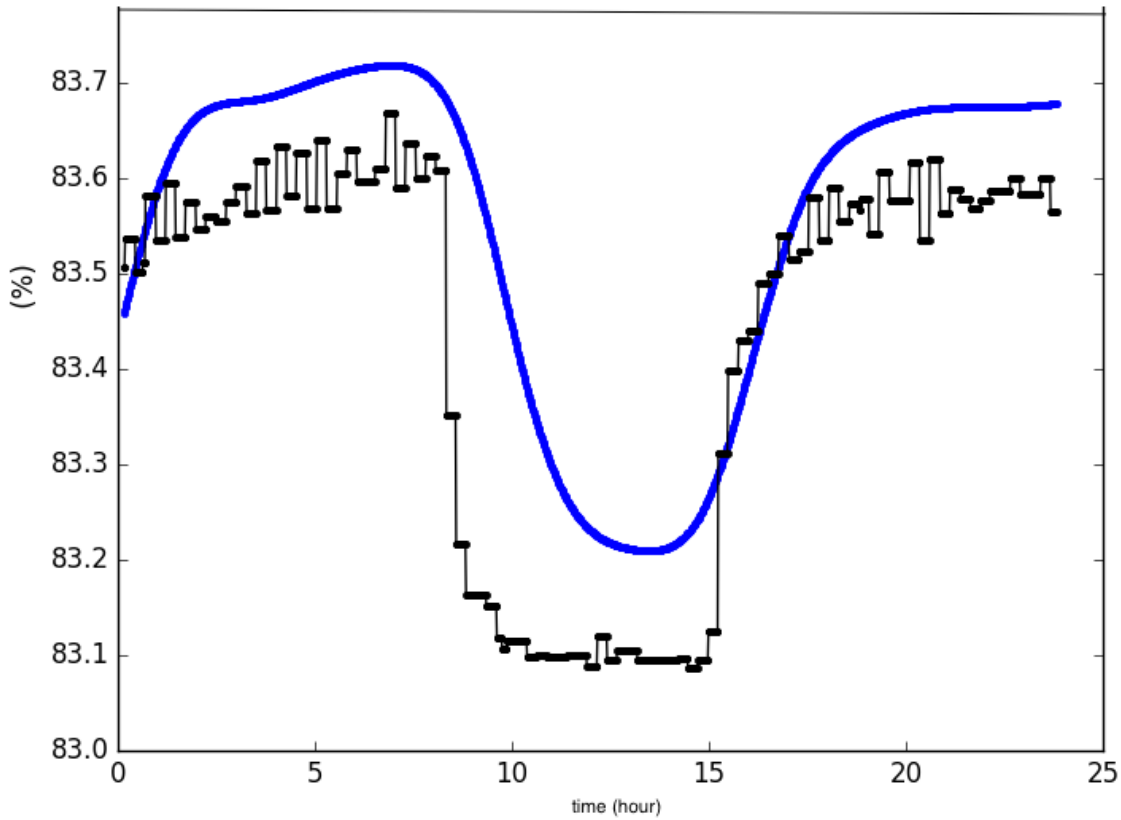

Figure: 100Y1 at node 5 for one day. Black: real measurement. Blue: computed.

THANK YOU FOR YOUR ATTENTION

Acknowledgments:

USC UNIVERSIDADE DE SANTIAGO DE COMPOSTELA

mat+i Grupo de Investigación en Ingeniería Matemática

ITMATI

reganosa

GOBIERNO DE ESPAÑA MINISTERIO DE ECONOMÍA Y COMPETITIVIDAD

European Union
European Regional Development Fund
"A way to build Europe"